

See discussions, stats, and author profiles for this publication at: <https://www.researchgate.net/publication/256187947>

# Synthesis, Resolution, and Biological Evaluation of Atropisomeric (aR)- and (aS)-16-Methyllamellarins N: Unique Effects of the Axial Chirality on the Selectivity of Protein Kinases...

ARTICLE *in* JOURNAL OF MEDICINAL CHEMISTRY · AUGUST 2013

Impact Factor: 5.45 · DOI: 10.1021/jm400719y · Source: PubMed

---

CITATIONS

6

READS

118

## 11 AUTHORS, INCLUDING:



Nadège Loäec

Station Biologique de Roscoff

19 PUBLICATIONS 97 CITATIONS

[SEE PROFILE](#)



Emilie Durieu

ManRos Therapeutics

23 PUBLICATIONS 192 CITATIONS

[SEE PROFILE](#)



Laurent Meijer

ManRos Therapeutics

411 PUBLICATIONS 20,756 CITATIONS

[SEE PROFILE](#)

# Synthesis, Resolution, and Biological Evaluation of Atropisomeric (aR)- and (aS)-16-Methylamellarins N: Unique Effects of the Axial Chirality on the Selectivity of Protein Kinases Inhibition

Kenyu Yoshida,<sup>†</sup> Ryosuke Itoyama,<sup>†</sup> Masashi Yamahira,<sup>‡</sup> Junji Tanaka,<sup>§</sup> Nadège Loaëc,<sup>||,⊥</sup> Olivier Lozach,<sup>||</sup> Emilie Durieu,<sup>||,⊥</sup> Tsutomu Fukuda,<sup>†</sup> Fumito Ishibashi,<sup>‡</sup> Laurent Meijer,<sup>||,⊥</sup> and Masatomo Iwao<sup>\*,†</sup>

<sup>†</sup>Division of Chemistry and Materials Sciences, Graduate School of Engineering, Nagasaki University, 1-14 Bunkyo-machi, Nagasaki 852-8521, Japan

<sup>‡</sup>Division of Marine Life Science and Biochemistry, Graduate School of Fisheries Science and Environmental Studies, Nagasaki University, 1-14 Bunkyo-machi, Nagasaki 852-8521, Japan

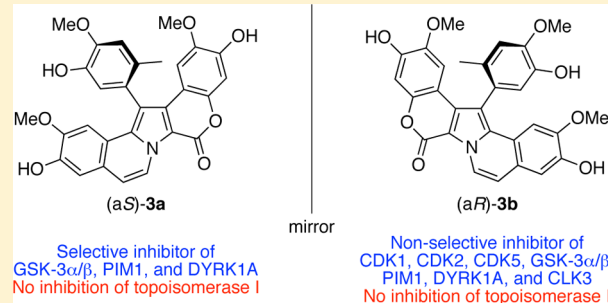
<sup>§</sup>Institute for Materials Chemistry and Engineering, Kyushu University, Kasuga Koen 6-1, Kasuga 816-8580, Japan

<sup>11</sup>Protein Phosphorylation and Human Disease Group, Station Biologique, CNRS, 29680 Roscoff, Bretagne, France

<sup>1</sup>ManRos Therapeutics, Centre de Perharidy, 290

## S Supporting Information

**ABSTRACT:** The total synthesis of the optically active (aR)- and (aS)-16-methyllamellarins N (**3a** and **3b**) was achieved via resolution on HPLC chiral stationary phase. The kinase inhibitory activities of both enantiomers were evaluated on eight protein kinases relevant to cancer and neurodegenerative diseases (CDK1/cyclin B, CDK2/cyclin A, CDK5/p25, GSK-3 $\alpha/\beta$ , PIM1, DYRK1A, CLK3, and CK1). Isomer (aR)-**3b** exhibited potent but nonselective inhibition on all protein kinases except CK1, while (aS)-**3a** selectively inhibited only GSK-3 $\alpha/\beta$ , PIM1, and DYRK1A. The different inhibition profiles of (aS)-**3a** and (aR)-**3b** were elucidated by docking simulation studies. Although parental lamellarin N (**2**) inhibited the action of topoisomerase I, both (aS)-**3a** and (aR)-**3b** showed no inhibition of this enzyme. The phenotypic cytotoxic activities of **2**, (aS)-**3a**, and (aR)-**3b** on three cancer cell lines (HeLa, SH-SY5Y, and IMR32) changed according to their topoisomerase I and protein kinase inhibitory activities.



## ■ INTRODUCTION

Lamellarins are unique marine polycyclic alkaloids sharing a common 14-phenyl-6*H*-[1]benzopyrano[4',3':4,5]pyrrolo[2,1-*a*]isoquinolin-6-one ring system.<sup>1–3</sup> Approximately 40 lamellarins have been isolated from a variety of marine organisms such as mollusks, ascidians, and sponges. These lamellarins differ in the number and position of the OH and OMe groups on their common scaffold (Figure 1). Lamellarins have received considerable attention owing to their interesting biological

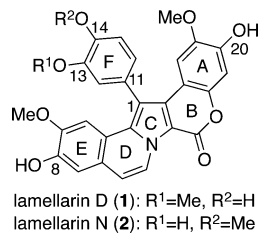


**Figure 1.** Structures of lamellarins D and N.

activities and potential development in various therapeutic areas.<sup>4,5</sup> For example, Quesada reported in 1996 that the triacetates of lamellarins D, N, and K showed potent cytotoxicity on P-glycoprotein-mediated MDR cancer cell lines as well as their respective parental cell lines at low nanomolar concentrations.<sup>6</sup> In addition, Faulkner reported in 1999 that lamellarin  $\alpha$  20-sulfate and related lamellarin sulfates inhibit HIV-1 integrase and display anti-HIV-1 activity.<sup>7-9</sup>

In 1997, we achieved the first total synthesis of lamellarin-class marine alkaloids (lamellarins D and H) by *N*-ylide mediated cyclization.<sup>10</sup> Using this method, we prepared a range of differentially substituted non-natural lamellarin D analogues and evaluated their cytotoxic activities on a HeLa cell line.<sup>11</sup> The SAR study indicated that the hydroxyl groups at the C8 and C20 positions of lamellarin D (**1**) are essential for its potent cytotoxicity, whereas the hydroxyl group at C14 is less important.<sup>11</sup> A more comprehensive SAR study conducted by

**Received:** May 14, 2013

**Published:** August 27, 2013

Ruchirawat and Ploypradith using a variety of cancer cell lines supports our results.<sup>12</sup> Concerning the mechanism of action, Bailly demonstrated that a major molecular target of **1** in cancer cells is DNA topoisomerase I.<sup>13</sup> They proposed a lamellarin D–DNA–topoisomerase I ternary complex model by docking simulation studies.<sup>14</sup> This model is in perfect agreement with our SAR study. Bailly also showed **1** could induce apoptosis of cancer cells through direct inhibition of mitochondrial function at micromolar concentrations.<sup>15,16</sup> Recently, we have reported that lamellarin N (**2**) strongly inhibits several protein kinases relevant to cancer and neurodegenerative diseases (Down syndrome, Alzheimer's disease, etc.) such as CDKs, GSK-3, PIM1, and DYRK1A.<sup>17</sup> A good correlation was observed between the effects of lamellarins on protein kinases and their action on cell death, suggesting that inhibition of specific kinases may contribute to the potent cytotoxicity of lamellarins.<sup>17</sup>

From a structural viewpoint, lamellarins are interesting because they possess axial chirality (atropisomerism) caused by restricted rotation around the C1–C11 single bond.<sup>18</sup> However, with the exception of lamellarin S,<sup>19</sup> all naturally occurring lamellarins isolated so far are optically inactive. In general, biological effects of enantiomers (optical isomers) are not identical owing to the chiral nature of the biological receptors.<sup>20</sup> Recently, the importance of axial chirality has been recognized in drug discovery.<sup>21–24</sup> In the case of lamellarins, however, all biological data reported so far were obtained from optically inactive compounds. Therefore, we decided to produce optically active lamellarins to elucidate relationships between their chiral structures and biological activities. In this paper, we describe the first resolution of a lamellarin class of the compound, 16-methyllamellarin N (**3**), and discuss the kinase inhibitory activities of the separated enantiomers (*aS*)-**3a** and (*aR*)-**3b** (Figure 2). Topoisomerase I inhibitory and cytotoxic activities of these compounds are also described.

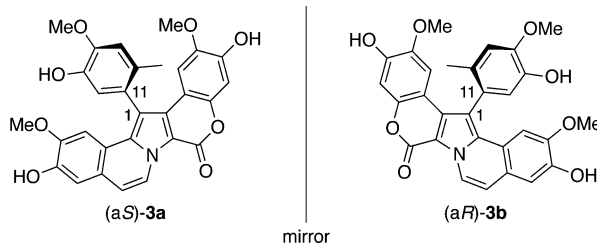


**Figure 2.** Enantiomers of axially chiral 16-methyllamellarin N.

## RESULTS AND DISCUSSION

**Synthesis and Attempted Resolution of O-Protected Lamellarins N.** We first attempted to prepare enantiomerically pure lamellarin N isomers via HPLC resolution using a chiral stationary phase. Since **2** is insoluble in most chromatographic solvents, we prepared different types of O-protected derivatives **8a–f** (Scheme 1). The known pentacyclic compound **4**<sup>25</sup> was brominated with NBS to give **5**. Suzuki–Miyaura coupling of **5** with boronic acid **6** under Qiu's conditions<sup>26</sup> [ $Pd(PPh_3)_4$  and  $CsF/Ag_2O$ ] provided **7** in good yield. DDQ dehydrogenation of **7** yielded **8a**. Deprotection of the isopropyl groups of **8a** with  $BCl_3$  led to **2**.<sup>27</sup> Tri-O-protected **8b–d** were prepared from **2** using appropriate reagents (**8b**,  $TBSCl/imidazole$ ; **8c**,  $Ac_2O/py$ ; **8d**,  $Boc_2O/DMAP$ ). Differentially protected **8e** was also synthesized from **5** by a cross-coupling with pinacol borate **9**

followed by dehydrogenation. Selective deprotection of the methoxymethyl (MOM) group of **8e** with  $HCl/MeOH$  provided partially protected **8f**.

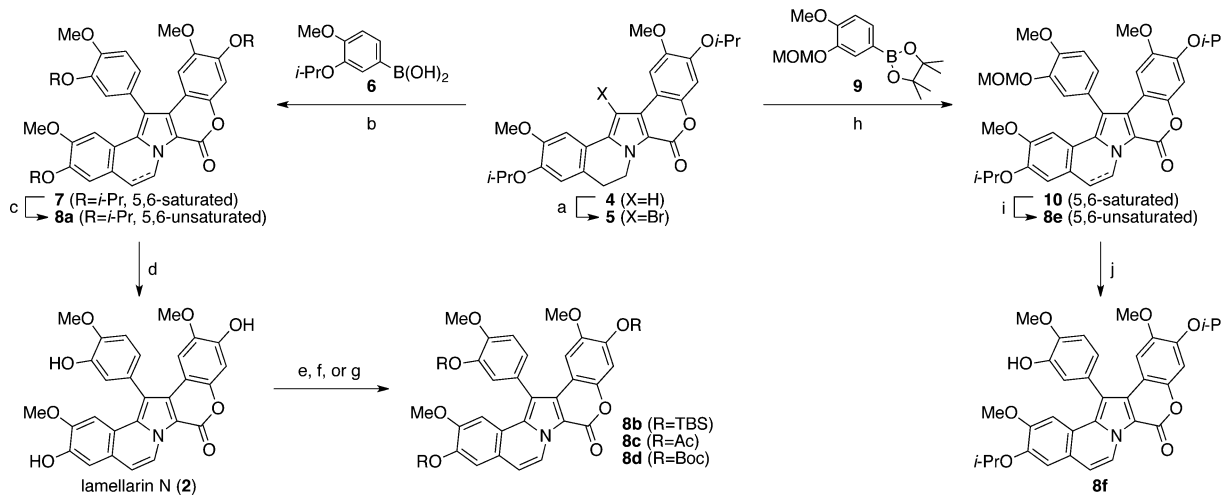
After producing O-protected lamellarins **N 8a–f**, we examined the chiral resolution of these compounds by HPLC. Although we tested a large variety of chiral stationary phases, the resolution of these compounds was unsuccessful. Several representative HPLC profiles are shown in Figure 3. These chromatographic patterns indicated that the separated enantiomers were racemized in HPLC columns.<sup>28</sup> Thus, the rotational energy barrier around the C1–C11 single bond of lamellarin was assumed to be lower than initially expected.<sup>18,29</sup>

**Synthesis and Resolution of 16-Methyllamellarin N.** We then attempted to resolve more sterically congested **3**. For the synthesis of **3**, Suzuki–Miyaura coupling of bromide **5** with boronic acid **11** was first examined. Although we tested a variety of conditions, the reaction was not successful in most cases owing to preferential formation of debrominated compound **4**. The desired cross-coupling product **12** was obtained in low yield only under Qiu's conditions<sup>26</sup> (Scheme 2). Insufficient formation of **12** is apparently due to severe steric hindrance of cross-coupling partners **5** and **11**. Thus, we designed a new synthetic route in which the cross-coupling was conducted at an earlier stage to avoid steric hindrance (Scheme 3). The known tricyclic lactone **13**<sup>25</sup> was alkylated with tosylate **14** to produce **15**. Reaction of **15** with NBS produced **16**, in which the  $\beta$ -position of the pyrrole ring was brominated regioselectively.<sup>25</sup> As expected, the cross-coupling of the less congested bromide **16** with boronic acid **11** smoothly proceeded to give **17** in good yield. Reaction of **17** with NBS produced bromide **18**. At this time, the pendent aromatic ring was brominated regioselectively.<sup>25</sup> Intramolecular Pd-catalyzed direct arylation<sup>30</sup> of **18** provided pentacyclic lamellarin **12** in good yield. DDQ dehydrogenation gave **5,6**-unsaturated **19**. Treatment of **19** with  $BCl_3$  gave racemic **3**.

O-Protected 16-methyllamellarin **N 19** was then converted to the optically active (*aS*)-**3a** and (*aR*)-**3b** (Scheme 4). As shown in Figure 4, racemic **19** was cleanly separated into optically pure **19a** and **19b** by HPLC using a CHIRALPAK IC semipreparative column. The CD spectra of **19a** and **19b**, shown in Figure 5, clearly indicate that these compounds are enantiomers of each other. The separated enantiomers were thermally stable and did not racemize even upon heating at 120 °C for 24 h in toluene. Selective deprotection of the isopropyl groups of **19a** and **19b** with  $BCl_3$  produced optically active (*aS*)-**3a** and (*aR*)-**3b**, respectively.

The absolute configurations of optically active 16-methyl-lamellarins **N** were then determined by X-ray crystallographic analysis. Because the anomalous dispersion effect of a heavy atom must be used for the determination of the absolute configuration, enantiomer **19b** was converted to its bromo derivative **21b** in two steps (Scheme 5). The X-ray crystallographic structure shown in Figure 6 clearly indicates that the absolute configuration of **21b** is *aS*. Thus, the absolute configurations of **19a** and **3a** are *aS*, and those of **19b** and **3b** are *aR*.

**Kinase Inhibitory Activity.** With enantiomerically pure (*aS*)-**3a** and (*aR*)-**3b** isolated, we evaluated the inhibitory pattern of these compounds on several protein kinases relevant to cancer and neurodegenerative diseases. The kinases tested were CDK1, CDK2, CDK5,<sup>31</sup> GSK-3 $\alpha/\beta$ ,<sup>32</sup> PIM1,<sup>33,34</sup> DYRK1A,<sup>35–38</sup> CLK3,<sup>39,40</sup> and CK1.<sup>41</sup> The  $IC_{50}$  values of **2**,<sup>17</sup> (*aS*)-**3a**, and (*aR*)-**3b** for these kinases are summarized in

Scheme 1. Synthesis of 8a–f<sup>a</sup>

<sup>a</sup>Reagents and conditions: (a) NBS, DMF, 0 °C, 89%; (b) 6, Pd(PPh<sub>3</sub>)<sub>4</sub>, CsF, Ag<sub>2</sub>O, DME, 85 °C, 80%; (c) DDQ, toluene, reflux, 97%; (d) BCl<sub>3</sub>, DCM, -78 to 0 °C, 97%; (e) TBSCl, imidazole, DMF, 0 °C to rt, 73%; (f) Ac<sub>2</sub>O, py, 0 °C to rt, 71%; (g) Boc<sub>2</sub>O, DMAP, TEA, MeCN, rt, 91%; (h) 9, Pd(PPh<sub>3</sub>)<sub>4</sub>, CsF, Ag<sub>2</sub>O, DME, 85 °C, 89%; (i) DDQ, DCM, reflux, 94%; (j) HCl, DCM-MeOH, 30 °C, 93%.

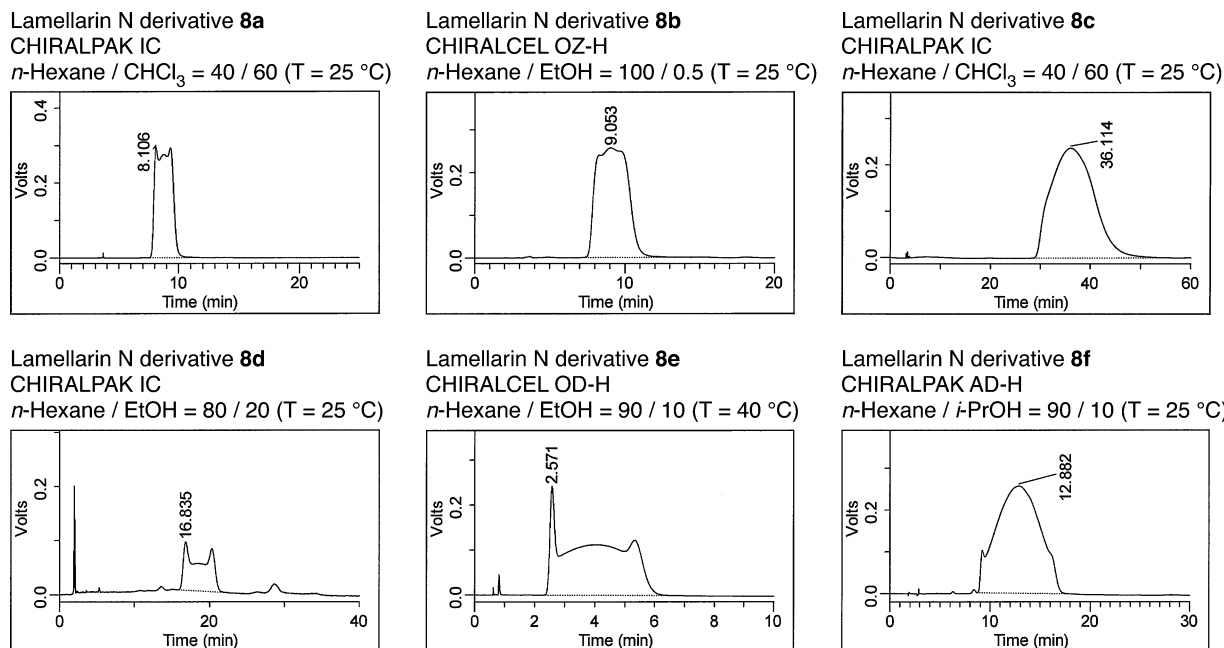
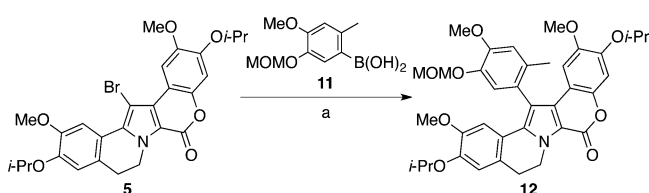


Figure 3. Selected HPLC profiles of 8a–f on chiral stationary phase columns.

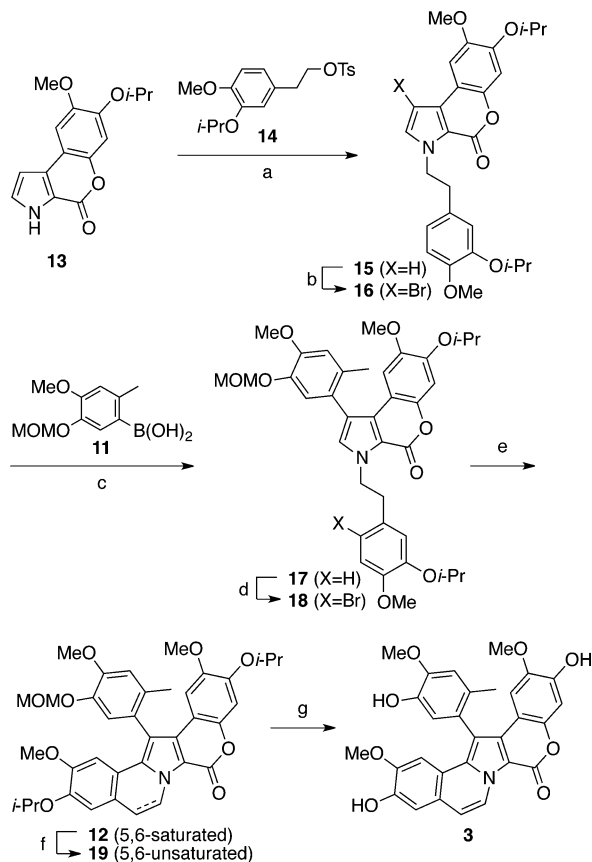
Scheme 2. Suzuki–Miyaura Coupling of 5 with 11<sup>a</sup>

<sup>a</sup>Reagents and conditions: (a) 11, Pd(PPh<sub>3</sub>)<sub>4</sub>, CsF, Ag<sub>2</sub>O, DME, 85 °C, 32%.

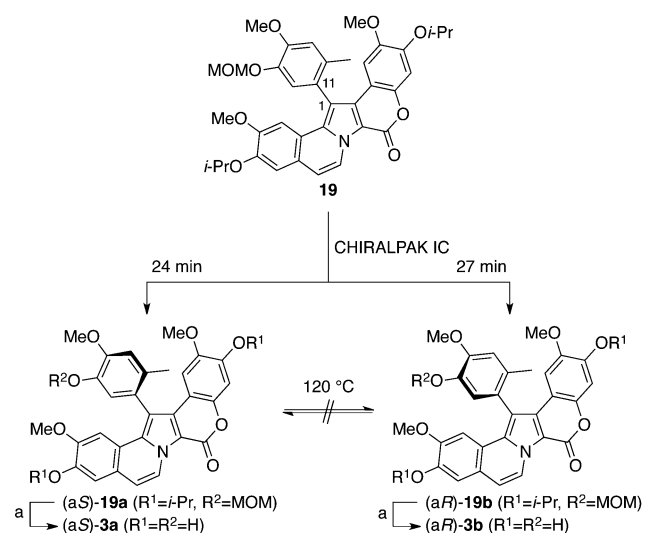
Table 1. (aR)-Isomer 3b strongly inhibited all protein kinases except CK1. This profile of potent and nonselective inhibition is similar to that of the parental 2. On the other hand, (aS)-isomer 3a selectively inhibited GSK-3 $\alpha/\beta$ , PIM1, and

DYRK1A. CDKs, CLK3, and CK1 were not inhibited with this enantiomer ( $IC_{50} > 10 \mu M$ ). The dramatic change in the inhibitory pattern caused by the axial chirality of 3 is quite striking. The selectivity observed for (aS)-3a is especially interesting from an application viewpoint.

**Docking Studies.** The results described above indicate that CDKs and CLK3 can discriminate the chiral structures of (aS)-3a and (aR)-3b, whereas GSK-3 $\alpha/\beta$ , PIM1, and DYRK1A cannot. To rationalize these observations, docking studies were performed. We selected CDK2 as the kinase that can discriminate (aS)-3a and (aR)-3b, and we selected GSK-3 $\beta$  as the kinase that cannot. For the docking simulations, CDK2/staurosporine<sup>42</sup> and GSK-3 $\beta$ /staurosporine<sup>43</sup> cocrystal structure data were employed because staurosporine and lamellarins share common structural features of planar and fused polyaromatic frameworks.<sup>44</sup> Thus, the ligand in the ATP-

Scheme 3. Synthesis of Racemic 3<sup>a</sup>

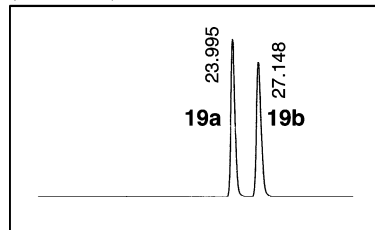
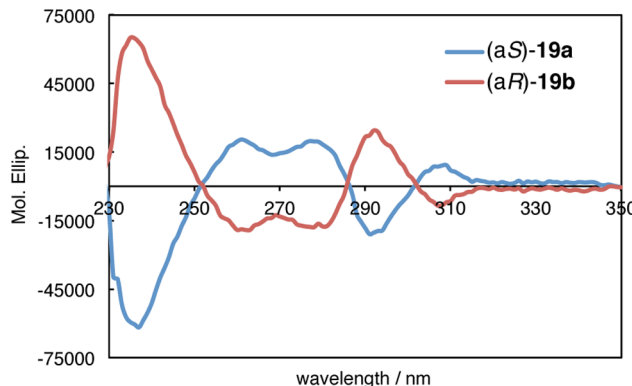
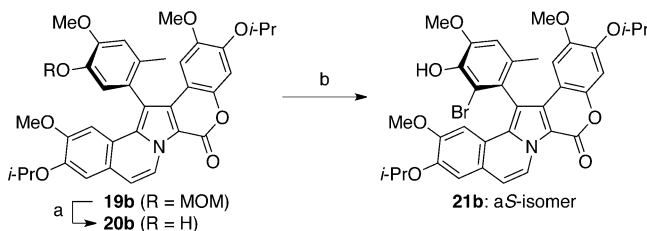
<sup>a</sup>Reagents and conditions: (a) 14,  $\text{Cs}_2\text{CO}_3$ , DMF, rt, 98%; (b) NBS, DMF, 0 °C to rt, 93%; (c) 11,  $\text{Pd}(\text{PPh}_3)_4$ , CsF,  $\text{Ag}_2\text{O}$ , DME, 85 °C, 80%; (d) NBS, THF, 0 °C to rt, 86%; (e)  $\text{Pd}(\text{PPh}_3)_4$ ,  $\text{K}_2\text{CO}_3$ , DMA, 125 °C, 87%; (f) DDQ, DCM, reflux, 99%; (g)  $\text{BCl}_3$ , DCM, -78 to 0 °C, 75%.

Scheme 4. Synthesis of Optically Active (*aS*)-3a and (*aR*)-3b by HPLC Resolution of 19<sup>a</sup>

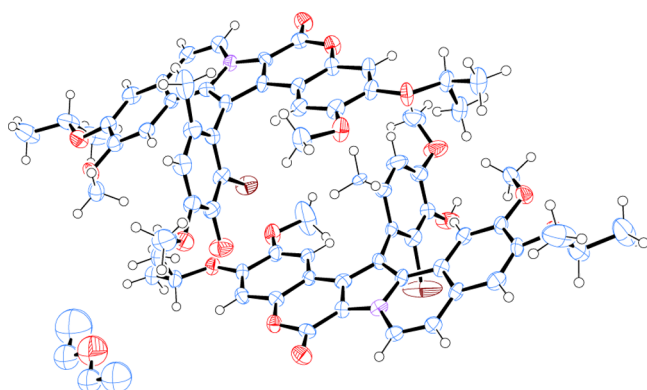
<sup>a</sup>Reagents and conditions: (a)  $\text{BCl}_3$ , DCM, -78 to 0 °C, (*aS*)-3a 99%, (*aR*)-3b 72%.

binding pocket of the staurosporine complexes was replaced by docking with **2**, (*aS*)-3a, and (*aR*)-3b, and the resulting

16-Methylamellarin N derivative **19**  
CHIRALPAK IC  
*n*-Hex /  $\text{CH}_2\text{Cl}_2$  / EtOH = 60 / 40 / 1  
(T = 25 °C)

Figure 4. HPLC profile of racemic **19** on a Chiralpac IC column.Figure 5. CD spectra of enantiomers **19a** and **19b**.Scheme 5. Synthesis of Bromide **21b**<sup>a</sup>

<sup>a</sup>Reagents and conditions: (a) HCl, DCM–MeOH, 30 °C, 92%; (b) NBS, DMF, 0 °C to rt, 92%.

Figure 6. X-ray crystal structure of **21b**.

complexes were minimized using the MOE program.<sup>45</sup> The models receiving the highest score are depicted in Figure 7 (CDK2 complexes) and Figure 8 (GSK-3 $\beta$  complexes).

**Table 1. Kinase Inhibitory Activities of 2, (aR)-3b, and (aS)-3a**

protein kinase	IC <sub>50</sub> (μM)		
	2 <sup>a</sup>	(aR)-3b	(aS)-3a
CDK1/cyclin B	0.070	0.052	>10
CDK2/cyclin A		0.067	>10
CDK5/p25	0.025	0.024	≥10
GSK-3α/β	0.005	0.21	0.37
PIM1	0.055	0.13	0.22
DYRK1A	0.035	0.042	0.44
CLK3		0.15	>10
CK1	>10	>10	>10

<sup>a</sup>Data from ref 17.

In CDK2–lamellarin N complex **22A**, the pentacyclic and planar lamellarin core is bound in the cleft between the N- and C-terminal lobes. The A ring is directed toward the solvent channel, and the E-ring is oriented to the specificity pocket.<sup>46</sup> The B-ring carbonyl forms a hydrogen bond with the NH of Leu83 located in the hinge region. The phenolic OH at C8 forms a hydrogen bond with the side chain of Asp145 located in the catalytic salt bridge. Additionally, the OH at C20 and the OMe at C21 chelatively interact with the side chain of Lys89. The phenolic OH at C13 of the F-ring is directed upward to Glu12 in the P-loop. There might be a favorable hydrogen-bonding interaction.<sup>47</sup>

The binding mode obtained for CDK2-(aR)-16-methyllamellarin N complex **22B** is quite similar to the parental **22A**. The bulky methyl group on the F-ring is appropriately accommodated in the hydrophobic cavity existing in the C-terminal lobe. Alternatively, in CDK2-(aS)-16-methyllamellarin N complex **22C**, the pentacyclic lamellarin core is rotated 180° compared to **22A** or **22B**. This unusual orientation of the

pentacyclic core is apparently less stable as shown by the scoring data (GBVI/WSA dG,<sup>48</sup> **22A**, -9.65 kcal/mol; **22B**, -9.78 kcal/mol; **22C**, -9.19 kcal/mol). Isomer (aS)-**3a** may not be able to take a normal and stable orientation of the pentacyclic core in the ATP-binding pocket because of severe steric repulsion between the 16-methyl group and the rigid β-sheet of the N-terminal lobe. These analyses clearly show why CDK2 discriminates between the axially chiral structures of 16-methyllamellarin N and allows us to present a rational explanation for the much lower activity of the (aS)-**3a** isomer over the (aR)-**3b** isomer.

The inability of GSK-3β to discriminate between the chiral structures of (aS)-**3a** and (aR)-**3b** is also clearly explained by comparing the docking models. The favorable orientation of **2** in the ATP-binding pocket of GSK-3β is similar to the orientation in that of CDK2. The A-ring is directed to the solvent channel, whereas the E-ring is directed to the specificity pocket. The B-ring carbonyl is hydrogen-bonded to the NH of Val135. The phenolic OH at C8 is also hydrogen-bonded to the salt bridge Asp200. Differing from the CDK2 complexes, the pentacyclic lamellarin cores of (aR)-**3b** and (aS)-**3a** in GSK-3β complexes **23B** and **23C** adopt an orientation similar to that observed in the parental complex **23A**. The scoring data assessed for **23B** and **23C** are very similar to each other, suggesting that the bulky 16-methyl group can direct upward or downward without any energetic preferences probably because of the larger capacity of the ATP-binding pocket of GSK-3β compared with that of CDK2. The similar inhibitory activity of (aS)-**3a** and (aR)-**3b** on GSK-3β can thus be explained by their similar binding abilities to the kinase target.

**Topoisomerase I Inhibitory Activity.** Compound **1** has been shown to be a potent inhibitor of topoisomerase I.<sup>13,14</sup> Therefore, we compared the topoisomerase I inhibitory activities of **1**, **2**, and chiral (aS)-**3a** and (aR)-**3b** using a

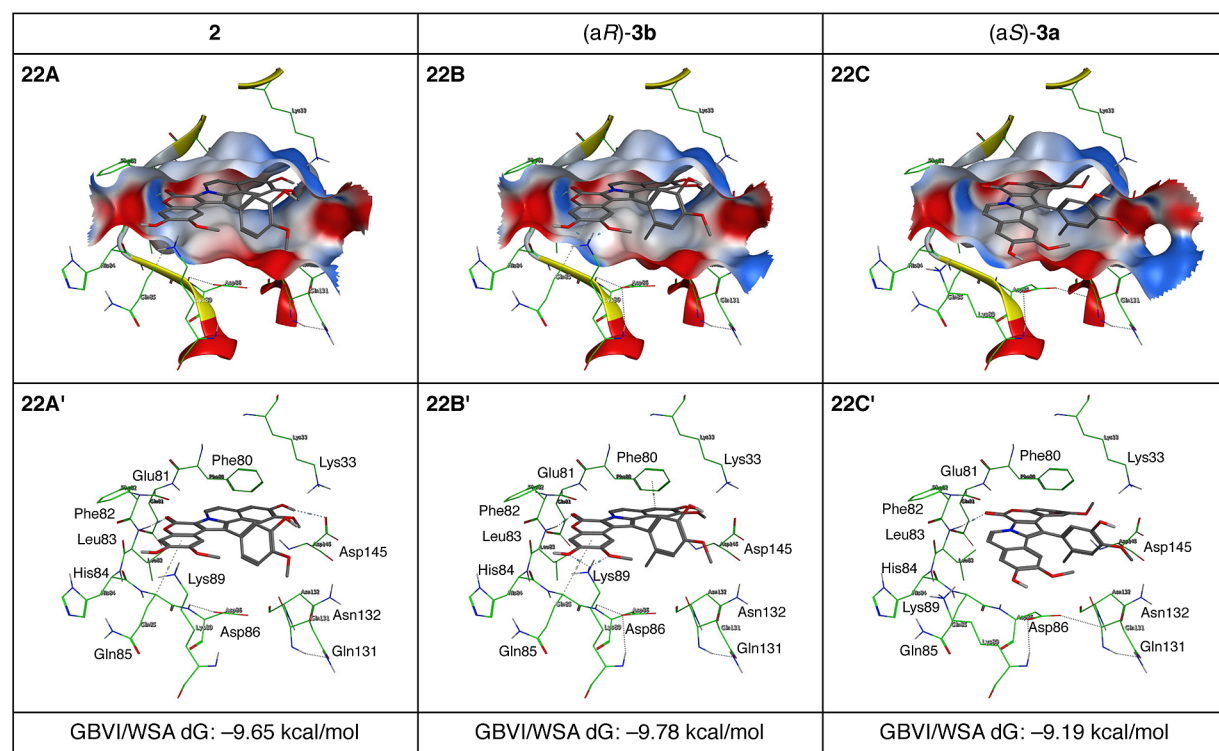


**Figure 7.** Highest score models obtained by docking of **2**, (aR)-**3b**, and (aS)-**3a** into ATP-binding pocket of CDK2.

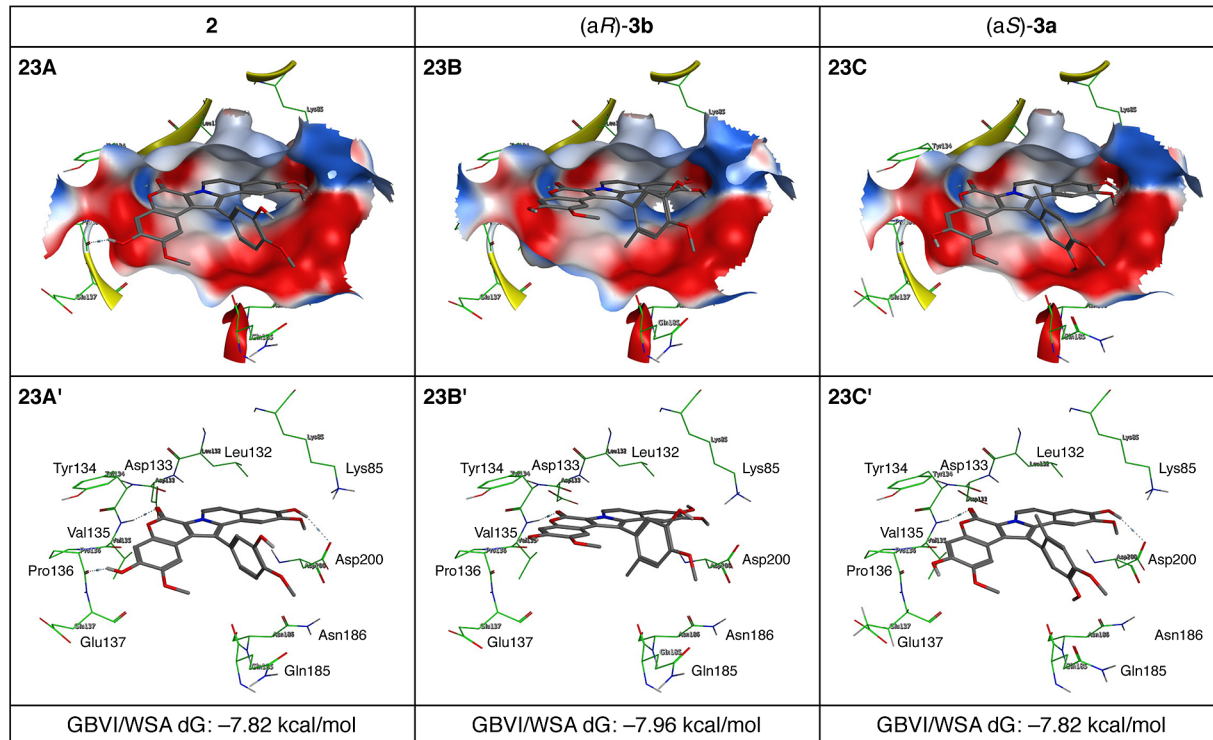


Figure 8. Highest score models obtained by docking of 2, (aR)-3b, and (aS)-3a into ATP-binding pocket of GSK-3 $\beta$ .

DNA relaxation assay.<sup>49</sup> The experiments were performed using three different concentrations of lamellarins (2, 10, and 50  $\mu$ M) (Figure 9). CPT was used as the reference compound at the same concentrations. The strong bands of nicked DNA observed at 50  $\mu$ M indicate that the topoisomerase I inhibitory activity of 1 is as potent as that of CPT. On the other hand, the activity of 2 is somewhat less potent than that of 1. Both enantiomers of (aS)-3a and (aR)-3b are completely inactive

even at 50  $\mu$ M. This interesting result may be accounted by considering the unfavorable steric interactions between the 16-methyl group of 3a or 3b and the base pairs of DNA, preventing the formation of a stable 3a (or 3b)–DNA–topoisomerase I ternary complex.<sup>14</sup>

**Cytotoxicity.** Finally, we compared the cytotoxicity of 2 and the chiral (aS)-3a and (aR)-3b on three different cancer cell lines (HeLa, SH-SY5Y, and IMR32). The results are shown in Table 2. The order of cytotoxicity on these cell lines is 2 > (aR)-

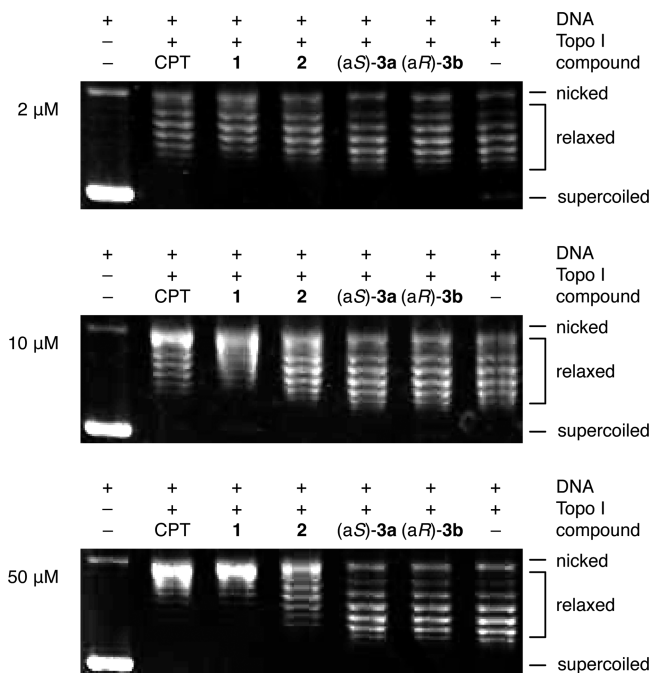


Figure 9. Topoisomerase I inhibition assay of lamellarins 1, 2, (aS)-3a, and (aR)-3b.

Table 2. Cell Survival/Proliferation Inhibitory Activities of 2, (aR)-3b, and (aS)-3a

cell line	IC <sub>50</sub> ( $\mu$ M)		
	2	(aR)-3b	(aS)-3a
HeLa <sup>a</sup>	0.032	0.160	2.95
SH-SY5Y <sup>b</sup>	0.040	0.79	4.1
IMR32 <sup>b</sup>	0.019	0.41	2.0

<sup>a</sup>Colony formation assay. <sup>b</sup>MTS assay.

3b > (aS)-3a. The lower cytotoxicity of (aS)-3a and (aR)-3b may be considered by the lack of their topoisomerase I inhibitory activity. The decreased cytotoxicity of (aS)-3a compared to (aR)-3b is likely due to the lack of CDK inhibitory activity of (aS)-3a.

## CONCLUSION

In this paper, we report the first successful synthesis and separation of axially chiral lamellarins, (aS)-3a and (aR)-3b, and also report the biological activities of the two enantiomers. The kinase inhibitory action of these enantiomers is quite different. Isomer (aR)-3b showed potent but nonselective inhibition of CDK1, CDK2, CDK5, GSK-3 $\alpha/\beta$ , PIM1, DYRK1A, and CLK3, whereas (aS)-3a exhibited selective inhibition of GSK-3 $\alpha/\beta$ ,

PIM1, and DYRK1A. These differences are rationalized by docking studies. Although parental 2 inhibited topoisomerase I, (aS)-3a and (aR)-3b were inactive on this enzyme. Thus, both (aS)-3a and (aR)-3b are the kinase-selective inhibitors. The different activities of 2, (aS)-3a, and (aR)-3b at the molecular level were reflected in their phenotypic cytotoxicity. The results obtained in this study open a new avenue in the chemical and pharmacological use of the lamellarin scaffold. Mastering the chirality of the C1–C11 single bond allows access to a subfamily of lamellarins. Lamellarins have been reported as potent kinase inhibitors;<sup>17</sup> however, they were rather broad spectrum inhibitors in terms of selectivity, and their pharmaceutical use was therefore limited. Starting from the lamellarin (aS)-3a isomer, we can envisage improving the potency of analogues toward the DYRK1A, GSK-3, and PIM1 kinases, all of which represent promising therapeutic targets for potent drugs to treat neurodegenerative diseases like Alzheimer's. The selection of the lamellarin (aS)-3a isomer removes inhibitory activities toward the cell cycle regulating CDKs and therefore associated antiproliferative and proapoptotic properties. This is an obvious advantage for the development of antineurodegenerative molecules. Studies on this new lamellarin scaffold are in progress in our laboratories.

## EXPERIMENTAL SECTION

**Synthesis: General.** Melting points are uncorrected. IR spectra are reported in terms of wavenumber of absorption ( $\text{cm}^{-1}$ ).  $^1\text{H}$  NMR spectra were recorded at 400 MHz and are reported relative to  $\text{Me}_4\text{Si}$  ( $\delta$  0.0). Data for  $^1\text{H}$  NMR spectra are reported as follows: chemical shift ( $\delta$  ppm), multiplicity, coupling constant (Hz), and integration.  $^{13}\text{C}$  NMR spectra were recorded at 100 MHz and are reported relative to  $\text{Me}_4\text{Si}$  ( $\delta$  0.0). Data for  $^{13}\text{C}$  NMR spectra are reported in terms of chemical shift. High resolution mass spectra were measured by the EI or FAB method. Elemental analysis was performed for C, H, and N. Column chromatography was conducted on silica gel 60N, 63–210  $\mu\text{m}$ , or Chromatorex NH-DM1020. Solvents were dried and distilled by standard methods if necessary.

**14-Bromo-3,11-diisopropoxy-2,12-dimethoxy-8,9-dihydro-6H-[1]benzopyrano[4',3':4,5]pyrrolo[2,1-a]isoquinolin-6-one (5).** A solution of NBS (151 mg, 0.848 mmol) in DMF (13 mL) was added dropwise to a solution of 4<sup>25</sup> (382 mg, 0.824 mmol) in DMF (10 mL) at 0 °C. The mixture was stirred for 24 h at 0 °C. The solution was diluted with water, and the product was extracted with DCM. The extract was washed with water and brine, dried over  $\text{Na}_2\text{SO}_4$ , and evaporated. The residue was purified by column chromatography over silica gel 60N (DCM–ethyl acetate = 20:1) to give 4 as a pale yellow solid (398 mg, 89%). Recrystallization from DCM–hexane gave a colorless powder. Mp 191.5–192.5 °C. IR (KBr): 1707, 1420, 1210, 1163, 1040  $\text{cm}^{-1}$ .  $^1\text{H}$  NMR (400 MHz,  $\text{CDCl}_3$ ):  $\delta$  1.43 (d,  $J$  = 6.1 Hz, 12H), 3.04 (t,  $J$  = 6.5 Hz, 2H), 3.95 (s, 3H), 3.96 (s, 3H), 4.58 (sep,  $J$  = 6.1 Hz, 1H), 4.63 (sep,  $J$  = 6.1 Hz, 1H), 4.71–4.78 (m, 2H), 6.83 (s, 1H), 6.91 (s, 1H), 8.14 (s, 1H), 8.20 (s, 1H).  $^{13}\text{C}$  NMR (100 MHz,  $\text{CDCl}_3$ ):  $\delta$  21.8, 22.1, 28.9, 42.6, 56.3, 56.3, 71.4, 86.6, 103.3, 104.8, 109.5, 109.7, 114.1, 114.7, 119.2, 127.1, 127.3, 135.3, 146.0, 146.6, 147.7, 148.1, 148.8, 154.8. Anal. Calcd for  $\text{C}_{27}\text{H}_{28}\text{BrNO}_6$ : C, 59.79; H, 5.20; N, 2.58. Found: C, 59.93; H, 5.09; N, 2.37.

**3,11-Diisopropoxy-14-(3-isopropoxy-4-methoxyphenyl)-2,12-dimethoxy-8,9-dihydro-6H-[1]benzopyrano[4',3':4,5]pyrrolo[2,1-a]isoquinolin-6-one (7).** Under an argon atmosphere, a mixture of 4 (84.6 mg, 0.156 mmol), 6 (59.3 mg, 0.282 mmol), CsF (57.2 mg, 0.377 mmol),  $\text{Ag}_2\text{O}$  (52.3 mg, 0.226 mmol), and  $\text{Pd}(\text{PPh}_3)_4$  (21.7 mg, 18.8  $\mu\text{mol}$ ) in DME (6 mL) was heated at 85 °C for 24 h. After cooling, the mixture was diluted with water and the product was extracted with DCM. The extract was washed with water and brine, dried over  $\text{Na}_2\text{SO}_4$ , and evaporated. The residue was purified successively by column chromatography over silica gel 60N (DCM–

ethyl acetate = 20:1) and column chromatography over Chromatorex NH-DM1020 (DCM–ethyl acetate = 20:1) to give 6 as a colorless solid (78.4 mg, 80%). Physical and spectroscopic data of this compound have been reported previously.<sup>27</sup>

**3,11-Diisopropoxy-14-(3-isopropoxy-4-methoxyphenyl)-2,12-dimethoxy-6H-[1]benzopyrano[4',3':4,5]pyrrolo[2,1-a]isoquinolin-6-one (8a).** Under an argon atmosphere, a mixture of 7 (78.4 mg, 0.125 mmol) and DDQ (42.5 mg, 0.187 mmol) in toluene (8.0 mL) was refluxed for 18 h. After cooling, the mixture was evaporated. The residue was purified by column chromatography over Chromatorex NH-DM1020 (hexane–ethyl acetate = 1:1) to give 8a as a colorless solid (75.6 mg, 97%). Physical and spectroscopic data of this compound have been reported previously.<sup>27</sup>

**3,11-Dihydroxy-14-(3-hydroxy-4-methoxyphenyl)-2,12-dimethoxy-6H-[1]benzopyrano[4',3':4,5]pyrrolo[2,1-a]isoquinolin-6-one (Lamellarin N) (2).** Under an argon atmosphere, a heptane solution of  $\text{BCl}_3$  (1.0 M, 719  $\mu\text{L}$ , 0.719 mmol) was added dropwise to a solution of 8a (100 mg, 0.160 mmol) in DCM (5.0 mL) at –78 °C. After being stirred for 30 min at this temperature, the reaction mixture was allowed to warm to room temperature and stirred for an additional 3 h. The mixture was quenched with saturated aqueous  $\text{NaHCO}_3$  and extracted with ethyl acetate. The extract was washed with brine, dried over  $\text{Na}_2\text{SO}_4$ , and evaporated. The residue was purified by column chromatography over silica gel 60N (acetone–methanol = 10:1) to give 2 as a pale gray powder (77.4 mg, 97%). Physical and spectroscopic data of this compound have been reported previously.<sup>27</sup>

**3,11-Bis(tert-butyldimethylsilyloxy)-14-[3-(tert-butyldimethylsilyloxy)-4-methoxyphenyl]-2,12-dimethoxy-6H-[1]benzopyrano[4',3':4,5]pyrrolo[2,1-a]isoquinolin-6-one (8b).**

To a mixture of 2 (30.0 mg, 0.0601 mmol) and TBSCl (40.7 mg, 0.270 mmol) in DMF (0.5 mL) was added imidazole (40.9 mg, 0.601 mmol) at 0 °C. After being stirred for 10 min at 0 °C, the mixture was allowed to warm to room temperature, stirred for 15 h at room temperature, and quenched with water. The product was extracted with DCM, and the extract was washed with water and brine, dried over  $\text{Na}_2\text{SO}_4$ , and evaporated. The residue was purified successively by column chromatography over silica gel 60N (DCM) and column chromatography over silica gel 60N (hexane–ethyl acetate = 10:1) to give 8b as a pale yellow solid (36.8 mg, 73%). Recrystallization from diethyl ether–hexane gave a colorless powder. Mp 241–242.5 °C. IR (KBr): 1710, 1432, 1283, 1218, 1157  $\text{cm}^{-1}$ .  $^1\text{H}$  NMR (400 MHz,  $\text{CDCl}_3$ ):  $\delta$  0.15 (s, 3H), 0.16 (s, 3H), 0.17 (s, 3H), 0.18 (s, 9H), 0.97 (s, 9H), 0.99 (s, 9H), 1.01 (s, 9H), 3.43 (s, 3H), 3.44 (s, 3H), 3.91 (s, 3H), 6.76 (s, 1H), 6.95 (s, 1H), 6.98 (d,  $J$  = 7.3 Hz, 1H), 7.10 (d,  $J$  = 2.0 Hz, 1H), 7.12 (s, 1H), 7.13 (d,  $J$  = 8.2 Hz, 1H), 7.18 (s, 1H), 7.20 (dd,  $J$  = 2.0 and 8.2 Hz, 1H), 9.21 (d,  $J$  = 7.3 Hz, 1H).  $^{13}\text{C}$  NMR (100 MHz,  $\text{CDCl}_3$ ):  $\delta$  –4.6, –4.6, –4.6, –4.6, –4.6, –4.5, 18.5, 18.5, 18.5, 25.7, 25.7, 54.8, 55.3, 56.0, 106.0, 106.1, 108.0, 109.6, 111.1, 111.4, 112.2, 113.1, 117.4, 120.1, 123.0, 124.1, 124.8, 124.9, 128.6, 129.3, 134.4, 145.8, 146.2, 146.4, 146.5, 147.8, 151.1, 151.3, 155.6. HREIMS  $m/z$  calcd for  $\text{C}_{46}\text{H}_{64}\text{NO}_8\text{Si}_3$  [(M + H)<sup>+</sup>]: 842.3940. Found: 842.3935.

**3,11-Bis(acetoxy)-14-(3-acetoxy-4-methoxyphenyl)-2,12-dimethoxy-6H-[1]benzopyrano[4',3':4,5]pyrrolo[2,1-a]isoquinolin-6-one (8c).** To a solution of 2 (29.6 mg, 0.0593 mmol) in pyridine (6.0 mL) was added acetic anhydride (25.2  $\mu\text{L}$ , 0.267 mmol) as a neat liquid at 0 °C. The mixture was allowed to warm to room temperature, stirred for 14.5 h at room temperature, and quenched with water. The product was extracted with DCM, and the extract was washed with 2 M aqueous HCl, water, and brine, dried over  $\text{Na}_2\text{SO}_4$ , and evaporated. The residue was purified by column chromatography over silica gel 60N (hexane–ethyl acetate = 3:1) to give 8c as a pale yellow solid (26.2 mg, 71%). Recrystallization from DCM–hexane gave a colorless powder. Mp 289–291 °C. IR (KBr): 1770, 1709, 1187, 1149, 1035  $\text{cm}^{-1}$ .  $^1\text{H}$  NMR (400 MHz,  $\text{CDCl}_3$ ):  $\delta$  2.32 (s, 3H), 2.32 (s, 3H), 2.34 (s, 3H), 3.48 (s, 6H), 3.93 (s, 3H), 6.78 (s, 1H), 7.02 (dd,  $J$  = 2.0 and 7.4 Hz, 1H), 7.13 (d,  $J$  = 2.0 Hz, 1H), 7.20 (s, 1H), 7.23 (d,  $J$  = 8.3 Hz, 1H), 7.33 (d,  $J$  = 2.1 Hz, 1H), 7.37 (s, 1H), 7.44 (dd,  $J$  = 2.1 and 8.3 Hz, 1H), 9.20 (dd,  $J$  = 2.0 and 7.4 Hz, 1H).  $^{13}\text{C}$  NMR (100 MHz,  $\text{CDCl}_3$ ):  $\delta$  20.5, 20.6, 20.6, 55.4, 55.6, 56.4, 106.2, 106.4, 109.0, 111.7, 112.1, 112.8, 113.2, 115.8, 120.7,

123.1, 123.8, 123.8, 125.9, 127.8, 128.5, 130.1, 133.8, 139.7, 140.9, 141.0, 145.5, 147.7, 151.0, 151.8, 155.1, 168.5, 168.7, 168.9. HREIMS  $m/z$  calcd for  $C_{34}H_{28}NO_{11}$  [(M + H) $^+$ ]: 626.1662. Found: 626.1664.

**3,11-Bis(tert-butoxycarbonyloxy)-14-[3-(tert-butoxycarbonyloxy)-4-methoxyphenyl]-2,12-dimethoxy-6H-[1]benzopyrano[4',3':4,5]pyrrolo[2,1-a]isoquinolin-6-one (8d).** To a mixture of **2** (30.0 mg, 0.0601 mmol), DMAP (6.0 mg, 0.0491 mmol), and TEA (37.6  $\mu$ L, 0.270 mmol) in MeCN (3.0 mL) was added  $Boc_2O$  (59.0 mg, 0.270 mmol) as a neat liquid. After being stirred for 17 h, the mixture was evaporated. The residue was purified by column chromatography over silica gel 60N (hexane–ethyl acetate = 1:1) to give **8d** as a pale yellow solid (43.6 mg, 91%). Recrystallization from DCM–hexane gave a colorless powder. Mp 197.5–198.5 °C. IR (KBr): 1760, 1710, 1255, 1141  $cm^{-1}$ .  $^1H$  NMR (400 MHz,  $CDCl_3$ ):  $\delta$  1.55 (s, 9H), 1.55 (s, 18H), 3.50 (s, 6H), 3.96 (s, 3H), 6.79 (s, 1H), 7.05 (d,  $J$  = 7.4 Hz, 1H), 7.21 (s, 1H), 7.23 (d,  $J$  = 8.3 Hz, 1H), 7.23 (s, 1H), 7.41 (dd,  $J$  = 2.1 and 8.3 Hz, 1H), 7.44 (d,  $J$  = 2.1 Hz, 1H), 7.47 (s, 1H), 9.23 (d,  $J$  = 7.4 Hz, 1H).  $^{13}C$  NMR (100 MHz,  $CDCl_3$ ):  $\delta$  27.6, 55.5, 55.8, 56.5, 83.7, 83.9, 84.0, 106.3, 106.5, 109.0, 111.7, 111.9, 112.8, 113.5, 115.7, 120.3, 123.2, 123.7, 123.8, 125.6, 127.8, 128.5, 130.1, 133.8, 140.1, 141.1, 141.4, 145.4, 147.9, 151.0, 151.1, 151.1, 151.9, 155.1. HREIMS  $m/z$  calcd for  $C_{43}H_{46}NO_{14}$  [(M + H) $^+$ ]: 800.2918. Found: 800.2938.

**3,11-Diisopropoxy-2,12-dimethoxy-14-[4-methoxy-3-(methoxymethoxy)phenyl]-8,9-dihydro-6H-[1]benzopyrano[4',3':4,5]pyrrolo[2,1-a]isoquinolin-6-one (10).** According to the procedure described for the preparation of **7**, compound **5** (30.0 mg, 55.3  $\mu$ mol), compound **9** (24.4 mg, 83.0  $\mu$ mol), CsF (16.8 mg, 0.111 mmol),  $Ag_2O$  (15.4 mg, 66.4  $\mu$ mol), and  $Pd(PPh_3)_4$  (6.4 mg, 5.5  $\mu$ mol) were reacted in DME (2.0 mL). After chromatographic purification over silica gel 60N (DCM–ethyl acetate = 20:1), **10** was obtained as a colorless solid (30.9 mg, 89%). Recrystallization from DCM–hexane gave a colorless powder. Mp 220.5–221.5 °C. IR (KBr): 1708, 1485, 1417, 1267, 1176  $cm^{-1}$ .  $^1H$  NMR (400 MHz,  $CDCl_3$ ):  $\delta$  1.37 (d,  $J$  = 6.1 Hz, 6H), 1.38 (d,  $J$  = 6.1 Hz, 6H), 3.09 (t,  $J$  = 6.8 Hz, 2H), 3.35 (s, 3H), 3.45 (s, 6H), 3.95 (s, 3H), 4.53 (sep,  $J$  = 6.1 Hz, 1H), 4.56 (sep,  $J$  = 6.1 Hz, 1H), 4.69–4.78 (m, 1H), 4.79–4.88 (m, 1H), 5.21 (d,  $J$  = 6.8 Hz, 1H), 5.23 (d,  $J$  = 6.8 Hz, 1H), 6.65 (s, 1H), 6.69 (s, 1H), 6.77 (s, 1H), 6.91 (s, 1H), 7.09 (d,  $J$  = 8.3 Hz, 1H), 7.16 (dd,  $J$  = 2.0 and 8.3 Hz, 1H), 7.33 (d,  $J$  = 2.0 Hz, 1H).  $^{13}C$  NMR (100 MHz,  $CDCl_3$ ):  $\delta$  21.8, 22.1, 28.7, 42.4, 55.1, 55.5, 56.2, 56.3, 71.3, 71.4, 95.6, 103.5, 105.0, 109.2, 110.4, 112.5, 113.7, 114.5, 114.7, 119.5, 120.2, 125.4, 126.4, 128.2, 128.3, 136.1, 146.0, 146.5, 147.0, 147.1, 147.3, 148.6, 149.7, 155.7. Anal. Calcd for  $C_{36}H_{39}NO_9$ : C, 68.67; H, 6.24; N, 2.22. Found: C, 68.41; H, 6.45; N, 2.14.

**3,11-Diisopropoxy-2,12-dimethoxy-14-[4-methoxy-3-(methoxymethoxy)phenyl]-6H-[1]benzopyrano[4',3':4,5]pyrrolo[2,1-a]isoquinolin-6-one (8e).** Under an argon atmosphere, a mixture of **10** (104 mg, 0.165 mmol) and DDQ (56.2 mg, 0.248 mmol) in DCM (7.0 mL) was refluxed for 24 h. After cooling, the mixture was evaporated. The residue was purified by column chromatography over Chromatorex NH-DM1020 (hexane–ethyl acetate = 1:1) to give **8e** as a colorless solid (97.5 mg, 94%). Recrystallization from DCM–hexane gave a colorless powder. Mp 200–201 °C. IR (KBr): 1700, 1432, 1423, 1264  $cm^{-1}$ .  $^1H$  NMR (400 MHz,  $CDCl_3$ ):  $\delta$  1.40 (d,  $J$  = 6.1 Hz, 6H), 1.43 (d,  $J$  = 6.1 Hz, 6H), 3.46 (s, 3H), 3.46 (s, 3H), 3.47 (s, 3H), 3.99 (s, 3H), 4.57 (sep,  $J$  = 6.1 Hz, 1H), 4.70 (sep,  $J$  = 6.1 Hz, 1H), 5.23 (d,  $J$  = 6.8 Hz, 1H), 5.25 (d,  $J$  = 6.8 Hz, 1H), 6.72 (s, 1H), 6.96 (s, 1H), 7.01 (d,  $J$  = 7.4 Hz, 1H), 7.09 (s, 1H), 7.15 (s, 1H), 7.17 (d,  $J$  = 8.2 Hz, 1H), 7.27 (dd,  $J$  = 2.0 and 8.2 Hz, 1H), 7.41 (d,  $J$  = 2.0 Hz, 1H), 9.21 (d,  $J$  = 7.4 Hz, 1H).  $^{13}C$  NMR (100 MHz,  $CDCl_3$ ):  $\delta$  21.8, 21.8, 21.9, 21.9, 55.1, 55.5, 56.3, 56.3, 71.2, 71.4, 95.7, 103.4, 105.6, 105.7, 107.8, 110.0, 110.4, 110.7, 112.3, 112.6, 119.0, 120.0, 123.2, 124.7, 125.9, 128.5, 129.5, 134.5, 146.5, 146.6, 147.3, 147.9, 148.5, 150.0, 150.2, 155.6. Anal. Calcd for  $C_{36}H_{37}NO_9$ : C, 68.89; H, 5.94; N, 2.23. Found: C, 68.75; H, 5.93; N, 2.22.

**14-(3-Hydroxy-4-methoxyphenyl)-3,11-diisopropoxy-2,12-dimethoxy-6H-[1]benzopyrano[4',3':4,5]pyrrolo[2,1-a]isoquinolin-6-one (8f).** To a mixture of **8e** (82.2 mg, 0.131 mmol), DCM (10 mL), and methanol (5.0 mL) was added concentrated HCl

(0.8 mL). After being stirred for 14 h at 30 °C, the mixture was diluted with water and evaporated. The product was extracted with DCM, and the extract was washed with water and brine, dried over  $Na_2SO_4$ , and evaporated. The residue was purified by column chromatography over silica gel 60N (hexane–ethyl acetate = 1:1) to give **8f** as a colorless solid (70.8 mg, 93%). Recrystallization from DCM–diethyl ether gave a colorless powder. Mp 241–242 °C (sealed capillary). IR (KBr): 1701, 1429, 1265, 1038  $cm^{-1}$ .  $^1H$  NMR (400 MHz,  $CDCl_3$ ):  $\delta$  1.40 (d,  $J$  = 6.1 Hz, 6H), 1.43 (d,  $J$  = 6.1 Hz, 6H), 3.46 (s, 3H), 3.48 (s, 3H), 4.00 (s, 3H), 4.57 (sep,  $J$  = 6.1 Hz, 1H), 4.69 (sep,  $J$  = 6.1 Hz, 1H), 5.91 (br s, 1H), 6.78 (s, 1H), 6.95 (s, 1H), 7.00 (d,  $J$  = 7.4 Hz, 1H), 7.08 (s, 1H), 7.10 (s, 1H), 7.11 (s, 1H), 7.19 (s, 1H), 7.21 (s, 1H), 9.20 (d,  $J$  = 7.4 Hz, 1H).  $^{13}C$  NMR (100 MHz,  $CDCl_3$ ):  $\delta$  21.8, 21.8, 21.9, 21.9, 55.1, 55.5, 56.4, 71.2, 71.5, 98.4, 103.4, 105.7, 105.8, 107.8, 110.0, 110.4, 110.9, 111.4, 112.3, 117.9, 119.0, 123.2, 123.5, 124.7, 129.0, 129.4, 134.4, 146.5, 146.5, 146.6, 146.6, 147.8, 148.4, 150.1, 155.6. HRFABMS  $m/z$  calcd for  $C_{34}H_{33}NO_8$  (M $^+$ ): 583.2206. Found: 583.2206.

**3,11-Diisopropoxy-2,12-dimethoxy-14-[4-methoxy-5-(methoxymethoxy)-2-methylphenyl]-8,9-dihydro-6H-[1]benzopyrano[4',3':4,5]pyrrolo[2,1-a]isoquinolin-6-one (12).** According to the procedure described for the preparation of **7**, compound **5** (30.0 mg, 55.3  $\mu$ mol), compound **11** (18.8 mg, 83.0  $\mu$ mol), CsF (16.8 mg, 0.111 mmol),  $Ag_2O$  (15.4 mg, 66.4  $\mu$ mol), and  $Pd(PPh_3)_4$  (6.4 mg, 5.5  $\mu$ mol) were reacted in DME (2.0 mL). After chromatographic purification over silica gel 60N (DCM–ethyl acetate = 20:1), **12** was obtained as a colorless solid (11.4 mg, 32%). Recrystallization from ethyl acetate gave a colorless powder. Mp 187–188 °C. IR (KBr): 1709, 1417, 1270, 1216, 1161  $cm^{-1}$ .  $^1H$  NMR (400 MHz,  $CDCl_3$ ):  $\delta$  1.38 (d,  $J$  = 6.1 Hz, 6H), 1.39 (d,  $J$  = 6.1 Hz, 6H), 2.07 (s, 3H), 3.11 (t,  $J$  = 6.8 Hz, 2H), 3.35 (s, 3H), 3.43 (s, 3H), 3.43 (s, 3H), 3.94 (s, 3H), 4.54 (sep,  $J$  = 6.1 Hz, 1H), 4.56 (sep,  $J$  = 6.1 Hz, 1H), 4.81 (t,  $J$  = 6.8 Hz, 2H), 5.15 (d,  $J$  = 6.7 Hz, 1H), 5.17 (d,  $J$  = 6.7 Hz, 1H), 6.53 (s, 1H), 6.67 (s, 1H), 6.77 (s, 1H), 6.92 (s, 1H), 6.97 (s, 1H), 7.21 (s, 1H).  $^{13}C$  NMR (100 MHz,  $CDCl_3$ ):  $\delta$  19.9, 21.8, 21.9, 22.1, 22.1, 28.6, 42.5, 55.1, 55.5, 56.1, 56.3, 71.3, 71.4, 95.8, 103.3, 104.4, 108.4, 110.6, 113.4, 113.9, 114.0, 114.6, 119.8, 120.4, 126.1, 126.9, 128.3, 132.9, 135.8, 145.1, 145.9, 146.7, 147.0, 147.3, 148.8, 149.9, 155.7. Anal. Calcd for  $C_{37}H_{41}NO_9$ : C, 69.04; H, 6.42; N, 2.18. Found: C, 69.08; H, 6.42; N, 2.13.

**2-(3-Isopropoxy-4-methoxyphenyl)ethyl p-Toluenesulfonate (14).** Under an argon atmosphere, *p*-toluenesulfonyl chloride (1.09 g, 5.71 mmol) in DCM (30 mL) was added dropwise to a solution of 2-(4-isopropoxy-3-methoxyphenyl)ethanol<sup>25</sup> (1.00 g, 4.76 mmol), DMAP (58.1 mg, 0.476 mmol), and triethylamine (729  $\mu$ L, 5.23 mmol) in DCM (30 mL) at 0 °C. The mixture was allowed to warm to room temperature and stirred for 13 h at room temperature and quenched with water. The product was extracted with DCM, and the extract was washed with water and brine, dried over  $Na_2SO_4$ , and evaporated. The residue was purified by column chromatography over silica gel 60N (hexane–ethyl acetate = 3:1) to give **14** as a colorless oil (1.47 g, 85%). IR (KBr): 1515, 1357, 1262, 1177, 1139  $cm^{-1}$ .  $^1H$  NMR (400 MHz,  $CDCl_3$ ):  $\delta$  1.33 (d,  $J$  = 6.1 Hz, 6H), 2.43 (s, 3H), 2.87 (t,  $J$  = 7.1 Hz, 2H), 3.82 (s, 3H), 4.17 (t,  $J$  = 7.1 Hz, 2H), 4.45 (sep,  $J$  = 6.1 Hz, 1H), 6.65 (dd,  $J$  = 2.1 and 8.7 Hz, 1H), 6.66 (d,  $J$  = 2.1 Hz, 1H), 6.76 (d,  $J$  = 8.7 Hz, 1H), 7.28 (d,  $J$  = 8.2 Hz, 2H), 7.69 (d,  $J$  = 8.2 Hz, 2H).  $^{13}C$  NMR (100 MHz,  $CDCl_3$ ):  $\delta$  21.6, 22.1, 34.9, 56.0, 70.9, 71.4, 112.0, 116.7, 121.5, 127.8, 128.6, 129.7, 133.0, 144.7, 147.2, 149.4. Anal. Calcd for  $C_{19}H_{24}O_5S$ : C, 62.61; H, 6.64. Found: C, 62.63; H, 6.80.

**7-Isopropoxy-3-[2-(3-isopropoxy-4-methoxyphenyl)ethyl]-8-methoxy[1]benzopyrano[3,4-b]pyrrol-4(3H)-one (15).** Under an argon atmosphere, a mixture of **13**<sup>25</sup> (614 mg, 2.25 mmol), **14** (1.29 g, 3.37 mmol), and  $Cs_2CO_3$  (2.19 g, 6.72 mmol) in DMF (20 mL) was stirred for 15 h at room temperature. The mixture was quenched with saturated aqueous  $NH_4Cl$  and diluted with water. The product was extracted with DCM, and the extract was washed with water and brine, dried over  $Na_2SO_4$ , and evaporated. The residue was purified by column chromatography over silica gel 60N (DCM–ethyl acetate = 20:1) to give **15** as a colorless solid (1.03 g, 98%). Physical

and spectroscopic data of this compound have been reported previously.<sup>25</sup>

**1-Bromo-7-isopropoxy-3-[2-(3-isopropoxy-4-methoxyphenyl)ethyl]-8-methoxy[1]benzopyrano[3,4-b]pyrrol-4(3H)-one (16).** According to the previously reported procedure,<sup>25</sup> compound 16 was synthesized. A solution of NBS (0.772 g, 4.34 mmol) in DMF (30 mL) was added dropwise to a solution of 15 (2.00 g, 4.29 mmol) in DMF (90 mL) at 0 °C. The mixture was stirred for 1 h at 0 °C and for 14 h at room temperature. The solution was diluted with water, and the product was extracted with DCM. The extract was washed with water and brine, dried over Na<sub>2</sub>SO<sub>4</sub>, and evaporated. The residue was purified by column chromatography over silica gel 60N (hexane–ethyl acetate = 3:1) to give 16 as a colorless solid (2.18 g, 93%). Physical and spectroscopic data of this compound have been reported previously.<sup>25</sup>

**7-Isopropoxy-3-[2-(3-isopropoxy-4-methoxyphenyl)ethyl]-8-methoxy-1-[4-methoxy-5-(methoxymethoxy)-2-methylphenyl][1]benzopyrano[3,4-b]pyrrol-4(3H)-one (17).** According to the procedure described for the preparation of 7, compound 16 (2.18 g, 4.00 mmol) was reacted with arylboronic acid 11 (1.81 g, 7.99 mmol). After chromatographic purification over silica gel 60N (hexane–ethyl acetate = 2:1), 17 was obtained as a colorless solid (2.07 g, 80%). Recrystallization from DCM–hexane gave a colorless powder. Mp 81–82 °C. IR (KBr): 1712, 1512, 1258, 1232, 1154 cm<sup>-1</sup>. <sup>1</sup>H NMR (400 MHz, CDCl<sub>3</sub>): δ 1.29 (d, J = 6.1 Hz, 3H), 1.29 (d, J = 6.1 Hz, 3H), 1.39 (d, J = 6.1 Hz, 3H), 1.40 (d, J = 6.1 Hz, 3H), 2.03 (s, 3H), 3.11 (dt, J = 3.1 and 6.8 Hz, 2H), 3.46 (s, 3H), 3.48 (s, 3H), 3.80 (s, 3H), 3.91 (s, 3H), 4.44 (sep, J = 6.1 Hz, 1H), 4.55 (sep, J = 6.1 Hz, 1H), 4.55–4.63 (m, 1H), 4.67–4.75 (m, 1H), 5.16 (d, J = 6.6 Hz, 1H), 5.19 (d, J = 6.6 Hz, 1H), 6.62 (s, 1H), 6.63 (dd, J = 2.0 and 8.2 Hz, 1H), 6.69 (s, 1H), 6.71 (d, J = 2.0 Hz, 1H), 6.75 (d, J = 8.2 Hz, 1H), 6.83 (s, 1H), 6.93 (s, 1H), 6.99 (s, 1H). <sup>13</sup>C NMR (100 MHz, CDCl<sub>3</sub>): δ 20.0, 21.8, 21.9, 22.0, 22.1, 37.6, 50.9, 55.7, 56.0, 56.1, 56.2, 71.4, 71.4, 95.8, 103.4, 104.5, 110.8, 112.1, 113.4, 114.6, 116.6, 117.3, 119.6, 121.5, 125.6, 128.1, 130.5, 131.8, 132.1, 144.2, 146.0, 146.8, 147.2, 147.3, 149.2, 149.6, 155.6. Anal. Calcd for C<sub>37</sub>H<sub>43</sub>NO<sub>9</sub>: C, 68.82; H, 6.71; N, 2.17. Found: C, 68.68; H, 6.83; N, 1.99.

**3-[2-(2-Bromo-5-isopropoxy-4-methoxyphenyl)ethyl]-7-isopropoxy-8-methoxy-1-[4-methoxy-5-(methoxymethoxy)-2-methylphenyl][1]benzopyrano[3,4-b]pyrrol-4(3H)-one (18).** A solution of NBS (0.577 g, 3.21 mmol) in THF (100 mL) was added dropwise to a solution of 17 (2.07 g, 3.21 mmol) in THF (100 mL) at 0 °C. The mixture was stirred for 15 h at 0 °C and for 24 h at room temperature. The solution was diluted with water, and the product was extracted with DCM. The extract was washed with water and brine, dried over Na<sub>2</sub>SO<sub>4</sub>, and evaporated. The residue was purified by column chromatography over silica gel 60N (hexane–ethyl acetate = 3:1) to give 18 as a colorless solid (2.00 g, 86%). Recrystallization from DCM–hexane gave a colorless powder. Mp 82.5–83.5 °C. IR (KBr): 1702, 1498, 1252, 1217, 1160 cm<sup>-1</sup>. <sup>1</sup>H NMR (400 MHz, CDCl<sub>3</sub>): δ 1.16 (d, J = 6.1 Hz, 3H), 1.19 (d, J = 6.1 Hz, 3H), 1.39 (d, J = 6.1 Hz, 3H), 1.40 (d, J = 6.1 Hz, 3H), 2.01 (s, 3H), 3.18–3.34 (m, 2H), 3.46 (s, 3H), 3.48 (s, 3H), 3.80 (s, 3H), 3.91 (s, 3H), 4.28 (sep, J = 6.1 Hz, 1H), 4.55 (sep, J = 6.1 Hz, 1H), 4.63–4.76 (m, 2H), 5.17 (d, J = 6.7 Hz, 1H), 5.19 (d, J = 6.7 Hz, 1H), 6.58 (s, 1H), 6.60 (s, 1H), 6.72 (s, 1H), 6.83 (s, 1H), 6.93 (s, 1H), 6.96 (s, 1H), 6.98 (s, 1H). <sup>13</sup>C NMR (100 MHz, CDCl<sub>3</sub>): δ 19.9, 21.8, 21.8, 21.8, 21.9, 37.6, 48.6, 55.7, 56.1, 56.1, 56.2, 71.4, 95.8, 103.4, 104.5, 110.8, 113.4, 114.3, 114.8, 115.9, 117.5, 117.6, 119.6, 125.5, 128.2, 129.1, 131.9, 132.1, 144.2, 146.0, 146.8, 146.8, 147.2, 149.6, 149.7, 155.6. Anal. Calcd for C<sub>37</sub>H<sub>42</sub>BrNO<sub>9</sub>: C, 61.33; H, 5.84; N, 1.93. Found: C, 61.05; H, 5.86; N, 1.84.

**3,11-Diisopropoxy-2,12-dimethoxy-14-[4-methoxy-5-(methoxymethoxy)-2-methylphenyl]-8,9-dihydro-6H-[1]benzopyrano[4',3':4,5]pyrrolo[2,1-a]isoquinolin-6-one (12).** Under an argon atmosphere, a mixture of 18 (2.00 g, 2.76 mmol), K<sub>2</sub>CO<sub>3</sub> (0.838 g, 6.06 mmol), and Pd(PPh<sub>3</sub>)<sub>4</sub> (0.159 g, 0.140 mmol) in DMA (54 mL) was heated at 125 °C for 20 h. After cooling to room temperature, the mixture was diluted with water and extracted with DCM. The extract was washed with water and brine, dried over

Na<sub>2</sub>SO<sub>4</sub>, and evaporated. The residue was purified by column chromatography over silica gel 60N (toluene–ethyl acetate = 5:1) to give 12 as a colorless solid (1.54 g, 87%).

**3,11-Diisopropoxy-2,12-dimethoxy-14-[4-methoxy-5-(methoxymethoxy)-2-methylphenyl]-6H-[1]benzopyrano[4',3':4,5]pyrrolo[2,1-a]isoquinolin-6-one (19).** According to the procedure described for the preparation of compound 8e, 12 (204 mg, 0.317 mmol) and DDQ (108 mg, 0.476 mmol) were reacted for 24 h. After chromatographic purification over Chromatorex NH-DM1020 (hexane–ethyl acetate = 2:1), 19 was obtained as a colorless solid (201 mg, 99%). Recrystallization from DCM–diethyl ether gave a colorless powder. Mp 195–196 °C. IR (KBr): 1702, 1423, 1267, 1209, 1179 cm<sup>-1</sup>. <sup>1</sup>H NMR (400 MHz, CDCl<sub>3</sub>): δ 1.41 (d, J = 6.1 Hz, 6H), 1.44 (d, J = 6.1 Hz, 6H), 2.08 (s, 3H), 3.43 (s, 3H), 3.45 (s, 3H), 3.46 (s, 3H), 3.98 (s, 3H), 4.58 (sep, J = 6.1 Hz, 1H), 4.71 (sep, J = 6.1 Hz, 1H), 5.17 (d, J = 6.7 Hz, 1H), 5.19 (d, J = 6.7 Hz, 1H), 6.66 (s, 1H), 6.98 (s, 1H), 7.04 (d, J = 7.4 Hz, 1H), 7.05 (s, 1H), 7.10 (s, 1H), 7.11 (s, 1H), 7.29 (s, 1H), 9.23 (d, J = 7.4 Hz, 1H). <sup>13</sup>C NMR (100 MHz, CDCl<sub>3</sub>): δ 19.9, 21.8, 21.9, 21.9, 55.2, 55.5, 56.2, 56.3, 71.1, 71.4, 95.9, 103.3, 105.0, 108.1, 109.6, 110.2, 110.3, 112.3, 114.0, 119.2, 120.3, 123.3, 124.7, 127.1, 129.3, 133.6, 134.2, 145.2, 146.6, 146.7, 147.9, 148.5, 150.1, 150.4, 155.6. Anal. Calcd for C<sub>37</sub>H<sub>43</sub>NO<sub>9</sub>: C, 69.25; H, 6.13; N, 2.18. Found: C, 68.95; H, 6.44; N, 1.94.

**3,11-Dihydroxy-14-(5-hydroxy-4-methoxy-2-methylphenyl)-2,12-dimethoxy-6H-[1]benzopyrano[4',3':4,5]pyrrolo[2,1-a]isoquinolin-6-one (3).** According to the procedure described for the preparation of 8a, compound 19 (30.0 mg, 46.8 μmol) was reacted with BCl<sub>3</sub> (1.0 M, 421 μL, 0.421 mmol). After chromatographic purification over silica gel 60N (ethyl acetate), 3 was obtained as a pale gray powder (17.9 mg, 75%). Mp 292–294 °C (sealed capillary). IR (KBr): 3377, 1679, 1433, 1275, 1148 cm<sup>-1</sup>. <sup>1</sup>H NMR (400 MHz, DMSO-d<sub>6</sub>): δ 1.99 (s, 3H), 3.40 (s, 3H), 3.41 (s, 3H), 3.88 (s, 3H), 6.67 (s, 1H), 6.89 (s, 1H), 6.90 (s, 1H), 7.10 (s, 1H), 7.18 (s, 1H), 7.22 (s, 1H), 7.24 (d, J = 7.4 Hz, 1H), 9.02 (d, J = 7.4 Hz, 1H), 9.14 (br s, 1H), 9.92 (br s, 2H). <sup>13</sup>C NMR (100 MHz, DMSO-d<sub>6</sub>): δ 19.0, 54.5, 55.0, 56.0, 103.6, 104.5, 105.0, 106.6, 108.3, 109.1, 111.4, 112.3, 114.8, 117.6, 118.1, 122.1, 124.5, 125.9, 128.5, 128.6, 133.6, 144.7, 145.5, 146.2, 147.8, 147.9, 148.3, 148.7, 154.3. HRFABMS m/z calcd for C<sub>29</sub>H<sub>23</sub>NO<sub>8</sub> (M<sup>+</sup>): 513.1424. Found: 513.1423.

**Resolution of 19.** The resolution was performed using HPLC with a Daicel semipreparative CHIRALPAK IC column (10 mm i.d. × 250 mm). The eluent was composed of n-hexane–DCM–ethanol (60:40:1, v/v/v). Flow rate was set at 2.0 mL/min, and detection wavelength was fixed at 305 nm. Racemate 19 (33.3 mg) was treated to give (aS)-19a (15.6 mg) and (aR)-19b (14.9 mg).

(aS)-3,11-Diisopropoxy-2,12-dimethoxy-14-[4-methoxy-5-(methoxymethoxy)-2-methylphenyl]-6H-[1]benzopyrano[4',3':4,5]pyrrolo[2,1-a]isoquinolin-6-one [(aS)-19a]. >99% ee. Mp 106–107.5 °C. [α]<sub>D</sub><sup>20</sup> -7.15 (c 0.695, CHCl<sub>3</sub>).

(aR)-3,11-Diisopropoxy-2,12-dimethoxy-14-[4-methoxy-5-(methoxymethoxy)-2-methylphenyl]-6H-[1]benzopyrano[4',3':4,5]pyrrolo[2,1-a]isoquinolin-6-one [(aR)-19b]. >99% ee. Mp 105.5–107.5 °C. [α]<sub>D</sub><sup>20</sup> +5.04 (c 0.745, CHCl<sub>3</sub>).

(aS)-3,11-Dihydroxy-14-(5-hydroxy-4-methoxy-2-methylphenyl)-2,12-dimethoxy-6H-[1]benzopyrano[4',3':4,5]pyrrolo[2,1-a]isoquinolin-6-one [(aS)-3a]. According to the procedure described for the preparation of 8a, compound 19a (30.0 mg, 46.8 μmol) was reacted with BCl<sub>3</sub> (1.0 M, 421 μL, 0.421 mmol). After chromatographic purification over silica gel 60N (ethyl acetate), (aS)-3a was obtained as a pale gray powder (23.7 mg, 99%). The enantiomeric excess of this compound was determined to be >99% ee by HPLC analysis (Daicel CHIRALCEL OD-H, hexane–2-propanol = 3:7) after conversion to the corresponding triacetate. Mp > 300 °C (sealed capillary). [α]<sub>D</sub><sup>20</sup> +3.6 (c 0.46, DMSO).

(aR)-3,11-Dihydroxy-14-(5-hydroxy-4-methoxy-2-methylphenyl)-2,12-dimethoxy-6H-[1]benzopyrano[4',3':4,5]pyrrolo[2,1-a]isoquinolin-6-one [(aR)-3b]. According to the procedure described for the preparation of 8a, compound 19b (30.0 mg, 46.8 μmol) was reacted with BCl<sub>3</sub> (1.0 M, 421 μL, 0.421 mmol). After chromatographic purification over silica gel 60N (ethyl acetate), (aR)-3b was obtained as a pale gray powder (88.0 mg, 72%). The

enantiomeric excess of this compound was determined to be >99% ee by HPLC analysis (Daicel Chiralcel OD-H, hexane–2-propanol = 3:7) after conversion to the corresponding triacetate. Mp > 300 °C (sealed capillary).  $[\alpha]_D^{20}$  −4.0 (*c* 0.46, DMSO).

**(aR)-14-(5-Hydroxy-4-methoxy-2-methylphenyl)-3,11-diisopropoxy-2,12-dimethoxy-6H-[1]benzopyrano[4',3':4,5]pyrrolo[2,1-a]isoquinolin-6-one [(aR)-20b].** According to the procedure described for the preparation of 8f, compound (aR)-19b (20.2 mg, 31.5  $\mu$ mol) was treated with concentrated HCl (0.4 mL) in a mixture of DCM (5.0 mL) and methanol (2.5 mL) for 8 h to give (aR)-20b as a colorless solid (17.3 mg, 92%). The enantiomeric excess of this compound was determined to be >99% ee by HPLC analysis (Daicel CHIRALPAK AD-H, hexane–2-propanol = 8:2). Recrystallization from DCM–hexane gave a colorless powder. Mp 217–219.5 °C (sealed capillary). IR (KBr): 3428, 1701, 1423, 1268, 1207  $\text{cm}^{-1}$ .  $^1\text{H}$  NMR (400 MHz,  $\text{CDCl}_3$ ):  $\delta$  1.41 (d, *J* = 6.1 Hz, 6H), 1.43 (d, *J* = 6.1 Hz, 6H), 2.05 (s, 3H), 3.46 (s, 3H), 3.47 (s, 3H), 3.98 (s, 3H), 4.58 (sep, *J* = 6.1 Hz, 1H), 4.70 (sep, *J* = 6.1 Hz, 1H), 5.71 (br s, 1H), 6.70 (s, 1H), 6.97 (s, 1H), 7.00 (s, 1H), 7.02 (d, *J* = 7.3 Hz, 1H), 7.09 (s, 1H), 7.10 (s, 1H), 7.13 (s, 1H), 9.22 (d, *J* = 7.3 Hz, 1H).  $^{13}\text{C}$  NMR (100 MHz,  $\text{CDCl}_3$ ):  $\delta$  19.8, 21.8, 21.9, 21.9, 21.9, 55.1, 55.5, 56.3, 71.2, 71.5, 103.3, 105.1, 105.2, 108.1, 109.7, 110.2, 110.3, 112.3, 112.7, 117.9, 119.2, 123.3, 124.6, 127.5, 129.2, 130.8, 134.1, 144.5, 146.6, 146.7, 146.7, 147.9, 148.5, 150.4, 155.7.  $[\alpha]_D^{20}$  −9.90 (*c* 0.675,  $\text{CHCl}_3$ ). HRFABMS *m/z* calcd for  $\text{C}_{35}\text{H}_{36}\text{NO}_8$  [(M + H) $^+$ ]: 598.2341, found 598.2439.

**(aS)-14-(2-Bromo-3-hydroxy-4-methoxy-6-methylphenyl)-3,11-diisopropoxy-2,12-dimethoxy-6H-[1]benzopyrano[4',3':4,5]pyrrolo[2,1-a]isoquinolin-6-one [(aS)-21b].** A solution of (aR)-20b (35.3 mg, 59.1  $\mu$ mol) in DMF (7.0 mL) was added dropwise to a solution of NBS (10.6 mg, 59.7  $\mu$ mol) in DMF (3.0 mL) at 0 °C. The mixture was stirred for 1 h at 0 °C and for 9 h at room temperature. The solution was diluted with water, and the product was extracted with ethyl acetate. The extract was washed with water and brine, dried over  $\text{Na}_2\text{SO}_4$ , and evaporated. The residue was purified by column chromatography over silica gel 60N (hexane–ethyl acetate = 1:1) to give (aS)-21b as a pale brown solid (36.9 mg, 92%). The enantiomeric excess of this compound was determined to be >99% ee by HPLC analysis (Daicel CHIRALPAK AD-H, hexane–2-propanol = 9:1). Recrystallization from DCM–diethyl ether gave pale brown granules. Mp 262.5–264.5 °C. IR (KBr): 3410, 1710, 1427, 1269, 1208  $\text{cm}^{-1}$ .  $^1\text{H}$  NMR (400 MHz,  $\text{CDCl}_3$ ):  $\delta$  1.41 (d, *J* = 6.1 Hz, 6H), 1.44 (d, *J* = 6.1 Hz, 6H), 2.05 (s, 3H), 3.45 (s, 3H), 3.47 (s, 3H), 4.02 (s, 3H), 4.59 (sep, *J* = 6.1 Hz, 1H), 4.71 (sep, *J* = 6.1 Hz, 1H), 6.03 (br s, 1H), 6.56 (s, 1H), 6.98 (s, 1H), 6.99 (s, 1H), 6.99 (s, 1H), 7.07 (d, *J* = 7.4 Hz, 1H), 7.12 (s, 1H), 9.25 (d, *J* = 7.4 Hz, 1H).  $^{13}\text{C}$  NMR (100 MHz,  $\text{CDCl}_3$ ):  $\delta$  21.0, 21.9, 21.9, 55.2, 55.6, 56.7, 71.2, 71.5, 103.3, 104.3, 104.6, 108.5, 108.5, 109.9, 110.2, 111.9, 112.5, 113.7, 119.0, 123.4, 124.8, 128.2, 129.2, 132.2, 134.0, 142.1, 146.7, 146.9, 147.1, 148.2, 148.7, 150.7, 155.6.  $[\alpha]_D^{20}$ +20.6 (*c* 0.700,  $\text{CHCl}_3$ ). HRFABMS *m/z* calcd for  $\text{C}_{35}\text{H}_{35}\text{BrNO}_8$  [(M + H) $^+$ ]: 676.1546. Found: 676.1561.

**X-ray Crystallographic Analysis of (aS)-21b.** Results are as follows: compound formula  $\text{C}_{38}\text{H}_{39}\text{BrNO}_8$ ,  $M_w$  = 717.63, monoclinic,  $P2_1$ ,  $a$  = 10.905(3) Å,  $b$  = 18.705(5) Å,  $c$  = 16.375(4) Å,  $\beta$  = 96.40(2)°,  $V$  = 3319(2)  $\text{\AA}^3$ ,  $Z$  = 4,  $D_{\text{calc}}$  = 1.436 g/cm<sup>3</sup>, monochromatized radiation  $\lambda$ (Cu  $\text{K}\alpha$ ) = 1.541 87 Å,  $\mu$  = 21.532 mm<sup>−1</sup>,  $F(000)$  = 1492.00,  $T$  = 113 K. Data were collected on a Rigaku RAXIS RAPID imaging plate to a  $\theta$  limit of 136.5° which yielded 41 261 reflections. There are 11 457 unique reflections with 8028 observed at the 2 $\sigma$  level. The structure was solved by direct methods (SIR92)<sup>50</sup> and refined using full-matrix least-squares on F2 (SHELXL-97).<sup>51</sup> The final model was refined using 849 parameters and all 11 457 data. All non-hydrogen atoms were refined with isotropic thermal displacements. The final agreement statistics are as follows:  $R$  = 0.0610 (based on 8028 reflections with  $I > 2\sigma(I)$ ),  $wR$  = 0.1512,  $S$  = 0.946. The maximum peak height in a final difference Fourier map is 1.19 e Å<sup>−3</sup>, and this peak is without chemical significance. The absolute configuration was determined based on the Flack parameter, −0.008(18), refined using 5230 Friedel pairs. CCDC 886003 contains the supplementary crystallographic data for this paper. These data can

be obtained free of charge from The Cambridge Crystallographic Data Centre via [www.ccdc.cam.ac.uk/data\\_request/cif](http://www.ccdc.cam.ac.uk/data_request/cif).

**Biological Assays: General.** The purity of all tested compounds [1, 2, (aS)-3a, and (aR)-3b] was determined to be >95% using HPLC with a Nacalai Cosmosil 5C<sub>18</sub>-AR-II column (4.6 mm i.d. × 250 mm). The eluent was composed of MeOH–H<sub>2</sub>O (70:30, v/v). Flow rate was set at 0.5 mL/min, and detection wavelength was fixed at 254 nm. CPT was purchased from TopoGEN, and its purity (>95%) was determined by HPLC as described above.

**Protein Kinase Inhibition Assays. Buffers.** Homogenization buffer consisted of 60 mM  $\beta$ -glycerophosphate, 15 mM *p*-nitrophenyl phosphate, 25 mM Mops (pH 7.2), 15 mM EGTA, 15 mM MgCl<sub>2</sub>, 1 mM DTT, 1 mM sodium vanadate, 1 mM NaF, 1 mM phenylphosphate, 10  $\mu$ g of leupeptin/mL, 10  $\mu$ g of aprotinin/mL, 10  $\mu$ g of soybean trypsin inhibitor/mL, and 100  $\mu$ M benzamidine. Buffer A consisted of 10 mM MgCl<sub>2</sub>, 1 mM EGTA, 1 mM DTT, 25 mM Tris-HCl, pH 7.5, and 50  $\mu$ g of heparin/mL.

**Kinase Preparations and Assays.** Kinase activities for each enzyme were assayed in buffer A, with their corresponding substrates, in the presence of 15  $\mu$ M ATP in a final volume of 30  $\mu$ L. After a 30 min incubation at 30 °C, the reaction was stopped by harvesting, using a FilterMate harvester (Packard), onto P81 phosphocellulose papers (GE Healthcare), which were washed in 1% phosphoric acid. Then 20  $\mu$ L of scintillation fluid was added and the radioactivity measured in a Packard counter. Blank values were subtracted and activities calculated as picomoles of phosphate incorporated during the 30 min incubation. The activities were expressed in % of the maximal activity, i.e., in the absence of inhibitors. Controls were performed with appropriate dilutions of DMSO.

CDK1/cyclin B was extracted in homogenization buffer from M phase starfish (*Marthasterias glacialis*) oocytes and purified by affinity chromatography on p9<sup>CKSh1</sup>-Sepharose beads, from which it was eluted by free p9<sup>CKSh1</sup> as previously described.<sup>52</sup> The kinase activity was assayed in buffer C, with 1 mg of histone H1/mL, in the presence of 15  $\mu$ M [ $\gamma$ -<sup>33</sup>P]ATP (3000 Ci/mmol, 10 mCi/mL) in a final volume of 30  $\mu$ L.

CDK2/cyclin A (human, recombinant, expressed in insect cells, from A. Echalier) was assayed as described for CDK1/cyclin B.

CDKS/p25 was reconstituted by mixing amounts of recombinant mammalian CDKS and p25 expressed in *E. coli* as GST (glutathione-S-transferase) fusion proteins and purified by affinity chromatography on glutathione-agarose (vectors kindly provided by Dr. L. H. Tsai) (p25 is a truncated version of p35, the 35 kDa CDKS activator). Its activity was assayed with histone H1 in buffer A as described for CDK1/cyclin B.

GSK-3 $\alpha/\beta$  was purified from porcine brain by affinity chromatography on immobilized axin.<sup>53</sup> It was assayed, following a 1/100 dilution in 1 mg BSA/mL of 10 mM DTT, with 5  $\mu$ L of 4  $\mu$ M GS-1 peptide substrate (GS-1, YRRAAVPPSPSLSRHSSPHQpSEDEEE where pS stands for phosphorylated serine), in buffer A, in the presence of 15  $\mu$ M [ $\gamma$ -<sup>33</sup>P]ATP (3000 Ci/mmol, 10 mCi/mL) in a final volume of 30  $\mu$ L.

PI3K was expressed as a GST-fusion protein in *E. coli* and purified by affinity chromatography on glutathione-agarose. Its kinase activity was assayed for 30 min with histone H1 in buffer C as described for CDK1/cyclin B.

DYRK1A (human, recombinant, expressed in *E. coli* as a GST fusion protein) was purified by affinity chromatography on glutathione-agarose and assayed as described for CDK1/cyclin B.

CLK3 (mouse, recombinant, and expressed in *E. coli* as GST fusion proteins) was assayed in buffer A (+0.15 mg BSA/mL) with RS peptide (GRSRSRSRSRSR) (1  $\mu$ g/assay).

CK1 $\delta/\epsilon$  was purified from porcine brain by affinity chromatography on an immobilized axin fragment.<sup>54</sup> It was assayed as described for CDK1 but using CKS (RRKHAAIGpSAYSITA), a CK1-specific peptide substrate.

**Topoisomerase I Inhibition Assay.** Topoisomerase I inhibition was assessed by measuring relaxation of supercoiled DNA pBR322 according to the reported method<sup>49</sup> with a slight modification. In brief, a mixture of 250 ng of plasmid pBR322 (Takara Bio, Inc.), 5 U

of calf thymus topoisomerase I (Takara Bio, Inc.), 1  $\mu$ L of a DMSO solution of the inhibitor, and 0.01% bovine serum albumin in topoisomerase I relaxation buffer (Takara Bio, Inc.) comprising 35 mM Tris-HCl (pH 8.0), 72 mM KCl, 5 mM MgCl<sub>2</sub>, 5 mM dithiothreitol, and 5 mM spermidine in final volume of 20  $\mu$ L was incubated at 37 °C for 30 min. The reaction was terminated by adding 2  $\mu$ L of 10% SDS solution followed by digestion with 2.2  $\mu$ L of proteinase K solution (TopoGEN, Inc.) at 0.5 mg/mL at 37 °C for 30 min. Then 2.4  $\mu$ L of 10× gel loading dye followed by 20  $\mu$ L of 24:1 chloroform/isoamyl alcohol (CIA) was added. The mixture was vortexed and centrifuged at 10 000 rpm at 4 °C for 1 min. The blue aqueous phase was applied to 1% agarose gel and electrophoresed for 2 h at 50 V/cm in Tris–borate–EDTA buffer containing 89 mM Tris, 89 mM H<sub>3</sub>BO<sub>4</sub>, and 2 mM Na EDTA. The gel was stained in 0.5  $\mu$ g/mL solution of ethidium bromide.

**Cytotoxicity Assay. Colony Formation Assay.** The cytotoxicity of test compounds was determined by the inhibitory activity of colony formation of HeLa cells as described previously.<sup>11</sup> In brief, 100–150 cells per well in a 24-well plate were cultured with varying concentrations of each test compound in the growth medium (MEM supplemented with streptomycin (100  $\mu$ g/mL), penicillin (100 U/mL), and 10% fetal calf serum) for 72 h at 37 °C under 5% CO<sub>2</sub>/95% air. The number of colonies formed was counted after staining with 1% methylene blue in 50% methanol. Clusters of 40 or more cells were considered as colonies. All assays were performed in duplicate with at least four different concentrations of the inhibitor, and the IC<sub>50</sub> values were calculated by least-squares fit to a logarithm-probit analysis. The IC<sub>50</sub> values (95% confidence limits) of **2**, (aS)-**3a**, and (aR)-**3b** thus obtained were 0.032 (0.028–0.037), 2.95 (1.57–9.02), and 0.16 (0.140–0.18)  $\mu$ M, respectively.

**MTS Assay.** SH-SY5Y or IMR32 human neuroblastoma cells were grown in DMEM supplemented with 2 mM L-glutamine (Invitrogen, Cergy Pontoise, France), plus antibiotics (penicillin–streptomycin) and 10% volume of fetal calf serum (FCS) (Invitrogen). Cell viability was determined by means of the MTS [3-(4,5-dimethylthiazol-2-yl)-5-(carbomethoxyphenyl)-2-(4-sulfonyl)-2H-tetrazolium] reduction method. All the assays were carried out in triplicate, and the values did not differ by more than 10%. The IC<sub>50</sub> values shown in Table 2 were estimated graphically from the dose–response curves performed with at least six concentrations of the inhibitor.

**Docking Simulation.** Docking studies were performed using MOE 2011.10.<sup>45</sup> Crystal structures of CDK2–staurosporine complex (PDB code 1AQ1)<sup>42</sup> and GSK-3 $\beta$ –staurosporine complex (PDB code 1Q3D)<sup>43</sup> were obtained from the Protein Data Bank. The protein structures for the docking were prepared by the following sequence: (i) A kinase–staurosporine complex was loaded. (ii) To the complex were added hydrogen atoms and electric charge by Protonate 3D (default settings). (iii) The hydrogen atoms were optimized by MMFF94x force field (the heavy atoms were fixed during the optimization). (iv) The dummy atoms were disposed in the docking site by Site Finder (default settings). On the other hand, the conformers of **2**, (aS)-**3a**, and (aR)-**3b** were obtained by conformational search using the LowModeMD search method with default parameters except for the following: the hydrogens check box was selected in order to include both hydrogen and heavy atoms in the rmsd calculation for duplication detection, and the value of energy window was set to 10 kcal/mol. Finally, the ligands were docked into the binding site of the kinases by using the Dock docking program according to the following sequence: (i) Initial poses were obtained using the Triangle Matcher placement (timeout, 3000 s; no. of return poses, 10 000), London dG resoring 1 (the maximum number of poses, 500), GridMin refinement (default settings), and GBVI/WSA dG<sup>48</sup> resoring 2 (the maximum number of poses, 100). (ii) The poses obtained in (i) were refined by force field refinement (default settings) and rescored by GBVI/WSA dG scoring function (the maximum number of poses, 100). (iii) The poses obtained in (ii) were refined by force field refinement (side chain, tether, the tether value was set to 10) and rescored by GBVI/WSA dG scoring function (the maximum number of poses, 100). (iv) The poses obtained in (iii) were refined by

force field refinement (side chain, free) and rescored by GBVI/WSA dG scoring function (the maximum number of poses, 100).

The obtained poses were evaluated using the GBVI/WSA dG scoring function, and the best scoring poses are shown in Figures 7 and 8.

## ASSOCIATED CONTENT

### S Supporting Information

Synthesis details of **11**, analytical data, and <sup>1</sup>H NMR and <sup>13</sup>C NMR spectra of all compounds synthesized in this work. This material is available free of charge via the Internet at <http://pubs.acs.org>.

## AUTHOR INFORMATION

### Corresponding Author

\*Phone: +81-95-819-2681. E-mail: iwao@nagasaki-u.ac.jp.

### Notes

The authors declare no competing financial interest.

## ACKNOWLEDGMENTS

This work was financially supported by a Grant-in-Aid for Scientific Research (B) (Grant No. 20310135) from the Japan Society for the Promotion of Science (JSPS). This research was supported by grants (L.M.) from the “Fonds Unique Interministériel” (FUI) PHARMASEA project, the “Association France-Alzheimer (Finistère)”, “CRITT-Santé Bretagne”, the “Cancéropôle Grand-Ouest”, the “Association France-Alzheimer Finistère”, the “Ligue Nationale contre le Cancer (Comité Grand-Ouest)”, the Fondation Jérôme Lejeune. This research was partly supported by an FP7-KBBE-2012 grant (BlueGenics) to L.M. The HPLC analyses shown in Figure 3 were performed at the laboratories of Daicel Corporation. We thank Daicel Corporation for these experiments.

## ABBREVIATIONS USED

CDK, cyclin-dependent kinase; GSK-3, glycogen synthase kinase 3; PIM-1, proto-oncogene serine/threonine-protein kinase Pim 1; DYRK1A, dual specificity, tyrosine phosphorylation regulated kinase 1A; CLK3, cdc2-like kinase 3; CK1, casein kinase 1; MDR, multidrug resistant; SAR, structure–activity relationship; TEA, triethylamine; DMA, dimethylacetamide; CPT, camptothecin; Topo I, topoisomerase I

## REFERENCES

- (1) Cironi, P.; Albericio, F.; Álvarez, M. Lamellarins: Isolation, Activity and Synthesis. *Prog. Heterocycl. Chem.* **2004**, *16*, 1–26.
- (2) Fan, H.; Peng, J.; Hamann, M. T.; Hu, J.-F. Lamellarins and Related Pyrrole-Derived Alkaloids from Marine Organisms. *Chem. Rev.* **2008**, *108*, 264–287.
- (3) Fukuda, T.; Ishibashi, F.; Iwao, M. Synthesis and Biological Activity of Lamellarin Alkaloids: An Overview. *Heterocycles* **2011**, *83*, 491–529.
- (4) Bailly, C. Lamellarins, from A to Z: A Family of Anticancer Marine Pyrrole Alkaloids. *Curr. Med. Chem.: Anti-Cancer Agents* **2004**, *4*, 363–378.
- (5) Kluza, J.; Marchetti, P.; Bailly, C. Lamellarin Alkaloids: Structure and Pharmacological Properties. In *Modern Alkaloids: Structure, Isolation, Synthesis and Biology*; Fattorusso, E., Taglialatela-Scafati, O., Eds.; Wiley-VCH: Weinheim, Germany, 2008; pp 171–187.
- (6) Quesada, A. R.; Grávalos, M. D. G.; Puentes, J. L. F. Polyaromatic Alkaloids from Marine Invertebrates as Cytotoxic Compounds and Inhibitors of Multidrug Resistance Caused by P-Glycoprotein. *Br. J. Cancer* **1996**, *74*, 677–682.

- (7) Reddy, M. V. R.; Rao, M. R.; Rhodes, D.; Hansen, M. S. T.; Rubins, K.; Bushman, F. D.; Venkateswarlu, Y.; Faulkner, D. J. Lamellarin  $\alpha$  20-Sulfate, an Inhibitor of HIV-1 Integrase Active against HIV-1 Virus in Cell Culture. *J. Med. Chem.* **1999**, *42*, 1901–1907.
- (8) Ridley, C. P.; Reddy, M. V. R.; Rocha, G.; Bushman, F. D.; Faulkner, D. J. Total Synthesis and Evaluation of Lamellarin  $\alpha$  20-Sulfate Analogs. *Bioorg. Med. Chem.* **2002**, *10*, 3285–3290.
- (9) Recently, we have indicated that the anti-HIV-1 activity of lamellarin sulfates is caused by inhibition of the virus entry step rather than the integration step. See the following: Kamiyama, H.; Kubo, Y.; Sato, H.; Yamamoto, N.; Fukuda, T.; Ishibashi, F.; Iwao, M. Synthesis, Structure–Activity Relationships, and Mechanism of Action of Anti-HIV-1 Lamellarin  $\alpha$  20-Sulfate Analogs. *Bioorg. Med. Chem.* **2011**, *19*, 7541–7550.
- (10) Ishibashi, F.; Miyazaki, Y.; Iwao, M. Total Syntheses of Lamellarin D and H. The First Synthesis of Lamellarin-Class Marine Alkaloids. *Tetrahedron* **1997**, *53*, 5951–5962.
- (11) Ishibashi, F.; Tanabe, S.; Oda, T.; Iwao, M. Synthesis and Structure–Activity Relationship Study of Lamellarin Derivatives. *J. Nat. Prod.* **2002**, *65*, 500–504.
- (12) Chittchang, M.; Batsomboon, P.; Ruchirawat, S.; Ploypradith, P. Cytotoxicities and Structure–Activity Relationships of Natural and Unnatural Lamellarins toward Cancer Cell Lines. *ChemMedChem* **2009**, *4*, 457–465.
- (13) Facompré, M.; Tardy, C.; Bal-Mahieu, C.; Colson, P.; Perez, C.; Manzanares, I.; Cuevas, C.; Bailly, C. Lamellarin D: A Novel Potent Inhibitor of Topoisomerase I. *Cancer Res.* **2003**, *63*, 7392–7399.
- (14) Marco, E.; Laine, W.; Tardy, C.; Lansiaux, A.; Iwao, M.; Ishibashi, F.; Bailly, C.; Gago, F. Molecular Determinants of Topoisomerase I Poisoning by Lamellarins: Comparison with Camptothecin and Structure–Activity Relationships. *J. Med. Chem.* **2005**, *48*, 3796–3807.
- (15) Kluza, J.; Gallego, M.-A.; Loyens, A.; Beauvillain, J.-C.; Sousa-Faro, J.-M. F.; Cuevas, C.; Marchetti, P.; Bailly, C. Cancer Cell Mitochondria Are Direct Proapoptotic Targets for the Marine Antitumor Drug Lamellarin D. *Cancer Res.* **2006**, *66*, 3177–3187.
- (16) Ballot, C.; Kluza, J.; Lancel, S.; Martoriat, A.; Hassoun, S. M.; Mortier, L.; Vienne, J.-C.; Briand, G.; Formstecher, P.; Bailly, C.; Nevière, R.; Marchetti, P. Inhibition of Mitochondrial Respiration Mediates Apoptosis Induced by the Anti-Tumoral Alkaloid Lamellarin D. *Apoptosis* **2010**, *15*, 769–781.
- (17) Baunbæk, D.; Trinkler, N.; Ferandin, Y.; Lozach, O.; Ploypradith, P.; Ruchirawat, S.; Ishibashi, F.; Iwao, M.; Meijer, L. Anticancer Alkaloid Lamellarins Inhibit Protein Kinases. *Marine Drugs* **2008**, *6*, 514–527.
- (18) Anderson, R. J.; Faulkner, D. J.; Cun-heng, H.; Van Duyne, G. D.; Clardy, J. Metabolites of the Marine Prosobranch Mollusk *Lamellaria* sp. *J. Am. Chem. Soc.* **1985**, *107*, 5492–5495.
- (19) Urban, S.; Capon, R. J. Lamellarin-S: A New Aromatic Metabolite from an Australian Tunicate, *Didemnum* sp. *Aust. J. Chem.* **1996**, *49*, 711–713.
- (20) Crossley, R. J. *Chirality and the Biological Activity of Drugs*; CRC Press: Boca Raton, FL, 1995.
- (21) Clayden, J.; Moran, W. J.; Edwards, P. J.; LaPlante, S. R. The Challenge of Atropisomerism in Drug Discovery. *Angew. Chem., Int. Ed.* **2009**, *48*, 6398–6401.
- (22) LaPlante, S. R.; Edwards, P. J.; Fader, L. D.; Jakalian, A.; Hucke, O. Revealing Atropisomer Axial Chirality in Drug Discovery. *ChemMedChem* **2011**, *6*, 505–513.
- (23) Takahashi, H.; Wakamatsu, S.; Tabata, H.; Oshitari, T.; Harada, A.; Inoue, K.; Natsugari, H. Atropisomerism Observed in Indometacin Derivatives. *Org. Lett.* **2011**, *13*, 760–763.
- (24) Tabata, H.; Nakagomi, J.; Morizono, D.; Oshitari, T.; Takahashi, H.; Natsugari, H. Atropisomerism in the Vaptan Class of Vasopressin Receptor Ligands: The Active Conformation Recognized by the Receptor. *Angew. Chem., Int. Ed.* **2011**, *50*, 3075–3079.
- (25) Ohta, T.; Fukuda, T.; Ishibashi, F.; Iwao, M. Design and Synthesis of Lamellarin D Analogs Targeting Topoisomerase I. *J. Org. Chem.* **2009**, *74*, 8143–8153.
- (26) Qiu, W.; Chen, S.; Sun, X.; Liu, Y.; Zhu, D. Suzuki Coupling Reaction of 1,6,7,12-Tetrabromoperylene Bisimide. *Org. Lett.* **2006**, *8*, 867–870.
- (27) Fujikawa, N.; Ohta, T.; Yamaguchi, T.; Fukuda, T.; Ishibashi, F.; Iwao, M. Total Synthesis of Lamellarins D, L, and N. *Tetrahedron* **2006**, *62*, 594–604.
- (28) Wolf, C. *Dynamic Stereochemistry of Chiral Compounds Principles and Applications*; The Royal Society of Chemistry: Cambridge, U.K., 2008; pp 136–179.
- (29) The rotational energy barriers around the C1–C11 single bond of O-protected lamellarins N were assumed to be around 83–87 kJ/mol by means of variable-temperature  $^1\text{H}$  and  $^{13}\text{C}$  NMR techniques. Fukuda, , T.; Itoyama, , R.; Minagawa, , T.; Iwao, , M. Rotational Energy Barrier around the C1–C11 Single Bond in Lamellarins: A Study by Variable-Temperature NMR. *Heterocycles* [Online early access]. DOI: DOI: 10.3987/COM-13-S(S)69. Published Online: Aug 26, 2013.
- (30) Alberico, D.; Scott, M. E.; Lautens, M. Aryl–Aryl Bond Formation by Transition-Metal-Catalyzed Direct Arylation. *Chem. Rev.* **2007**, *107*, 174–238.
- (31) Knockaert, M.; Greengard, P.; Meijer, L. Pharmacological Inhibitors of Cyclin-Dependent Kinases. *Trends Pharmacol. Sci.* **2002**, *23*, 417–425.
- (32) Meijer, L.; Flajolet, M.; Greengard, P. Pharmacological Inhibitors of Glycogen Synthase Kinase 3. *Trends Pharmacol. Sci.* **2004**, *25*, 471–480.
- (33) Bachmann, M.; Möröy, T. The Serine/Threonine Kinase Pim-1. *Int. J. Biochem. Cell Biol.* **2005**, *37*, 726–730.
- (34) Wang, J.; Anderson, P. D.; Luo, W.; Gius, D.; Roh, M.; Abdulkadir, S. A. Pim1 Kinase Is Required To Maintain Tumorigenicity in MYC-Expressing Prostate Cancer Cells. *Oncogene* **2012**, *31*, 1794–1803.
- (35) Tejedor, F. J.; Hä默le, B. MNB/DYRK1A as a Multiple Regulator of Neuronal Development. *FEBS J.* **2011**, *278*, 223–235.
- (36) Wegiel, J.; Gong, C.-X.; Hwang, Y.-W. The Role of DYRK1A in Neurodegenerative Diseases. *FEBS J.* **2011**, *278*, 236–245.
- (37) Becker, W.; Sippl, W. Activation, Regulation, and Inhibition of DYRK1A. *FEBS J.* **2011**, *278*, 246–256.
- (38) Tahtouh, T.; Elkins, J. M.; Filippakopoulos, P.; Soundararajan, M.; Burg, G.; Durieu, E.; Cochet, C.; Schmid, R. S.; Lo, D. C.; Delhommel, F.; Oberholzer, A. E.; Pearl, L. H.; Carreaux, F.; Bazureau, J.-P.; Knapp, S.; Meijer, L. Selectivity, Cocrystal Structures, and Neuroprotective Properties of Leucettines, a Family of Protein Kinase Inhibitors Derived from the Marine Sponge Alkaloid Leucettamine B. *J. Med. Chem.* **2012**, *55*, 9312–9330.
- (39) Duncan, P. I.; Stojdl, D. F.; Marius, R. M.; Scheit, K. H.; Bell, J. C. The Clk2 and Clk3 Dual-Specificity Protein Kinases Regulate the Intracellular Distribution of SR Proteins and Influence Pre-mRNA Splicing. *Exp. Cell Res.* **1998**, *241*, 300–308.
- (40) Muraki, M.; Ohkawara, B.; Hosoya, T.; Onogi, H.; Koizumi, J.; Koizumi, T.; Sumi, K.; Yomoda, J.; Murray, M. V.; Kimura, H.; Furuchi, K.; Shibuya, H.; Krainer, A. R.; Suzuki, M.; Hagiwara, M. Manipulation of Alternative Splicing by a Newly Developed Inhibitor of Clks. *J. Biol. Chem.* **2004**, *279*, 24246–24254.
- (41) Knippschild, U.; Wolff, S.; Giamas, G.; Brockschmidt, C.; Wittau, M.; Wür, P. U.; Eismann, T.; Stöter, M. The Role of the Casein Kinase 1 (CK1) Family in Different Signaling Pathways Linked to Cancer Development. *Oncologie* **2005**, *28*, 508–514.
- (42) Lawrie, A. M.; Noble, M. E. M.; Tunnah, P.; Brown, N. R.; Johnson, L. N.; Endicott, J. A. Protein Kinase Inhibition by Staurosporine Revealed in Details of the Molecular Interaction with CDK2. *Nat. Struct. Biol.* **1997**, *4*, 796–801.
- (43) Bertrand, J. A.; Thieffine, S.; Vulpetti, A.; Cristiani, C.; Valsasina, B.; Knapp, S.; Kalisz, H. M.; Flocco, M. Structural Characterization of the GSK-3 $\beta$  Active Site Using Selective and Non-Selective ATP-Mimetic Inhibitors. *J. Mol. Biol.* **2003**, *333*, 393–407.
- (44) It is noteworthy that staurosporine derivatives and lamellarins were isolated from the similar prosobranch mollusks of the *Coriocella* family. See the following: Cantrell, C. L.; Graweiss, A.; Gustafson, K.

R.; Boyd, M. R. A New Staurosporine Analog from the Prosobranch Mollusk *Coriocella nigra*. *Nat. Prod. Lett.* **1999**, *14*, 39–46.

(45) *Molecular Operating Environment (MOE)*, version 2011.10; Chemical Computing Group Inc.: Montreal, Quebec, Canada, 2011; <http://www.chemcomp.com>.

(46) Ghose, A. K.; Herbertz, T.; Pippin, D. A.; Salvino, J. M.; Mallamo, J. P. Knowledge Based Prediction of Ligand Binding Modes and Rational Inhibitor Design for Kinase Drug Discovery. *J. Med. Chem.* **2008**, *51*, S149–S171.

(47) Echalier, A.; Bettayeb, K.; Ferandin, Y.; Lozach, O.; Clément, M.; Valette, A.; Liger, F.; Marquet, B.; Morris, J. C.; Endicott, J. A.; Joseph, B.; Meijer, L. Meriolins (3-(Pyrimidin-4-yl)-7-azaindoles): Synthesis, Kinase Inhibitory Activity, Cellular Effects, and Structure of a CDK2/Cyclin A/Meriolin Complex. *J. Med. Chem.* **2008**, *51*, 737–751.

(48) Corbeil, C. R.; Williams, C. I.; Labute, P. Variability in Docking Success Rates Due to Dataset Preparation. *J. Comput.-Aided Mol. Des.* **2012**, *26*, 775–786.

(49) Liu, L. F.; Miller, K. G. Eukaryotic DNA Topoisomerases: Two Forms of Type I DNA Topoisomerases from HeLa Cell Nuclei. *Proc. Natl. Acad. Sci. U.S.A.* **1981**, *78*, 3487–3491.

(50) Altomare, A.; Cascarano, G.; Giacovazzo, C.; Guagliardi, A.; Burla, M. C.; Polidori, G.; Camalli, M. SIR 92—A Program for Automatic Solution of Crystal Structures by Direct Methods. *J. Appl. Crystallogr.* **1994**, *27*, 435.

(51) Sheldrick, G. M. A Short History of SHELX. *Acta Crystallogr., Sect. A: Found. Crystallogr.* **2008**, *64*, 112–122.

(52) Meijer, L.; Borgne, A.; Mulner, O.; Chong, J. P. J.; Blow, J. J.; Inagaki, N.; Inagaki, M.; Delcros, J.-G.; Moulinoux, J.-P. Biochemical and Cellular Effects of Roscovitine, a Potent and Selective Inhibitor of the Cyclin-Dependent Kinases cdc2, cdk2 and cdk5. *Eur. J. Biochem.* **1997**, *243*, 527–536.

(53) Primot, A.; Baratte, B.; Gompel, M.; Borgne, A.; Liabeuf, S.; Romette, J.-L.; Jho, E.; Costantini, F.; Meijer, L. Purification of GSK-3 by Affinity Chromatography on Immobilized Axin. *Protein Expression Purif.* **2000**, *20*, 394–404.

(54) Reinhardt, J.; Ferandin, Y.; Meijer, L. Purification of CK1 by Affinity Chromatography on Immobilised Axin. *Protein Expression Purif.* **2007**, *54*, 101–109.